

Sensory and Motor Systems

# The Contribution of Premotor Cortico-Striatal Projections to the Execution of Serial Order Sequences

Asai Sánchez-Fuentes, Kathia I. Ramírez-Armenta, Anil Kumar Verma-Rodríguez, Edgar Díaz-Hernández, Antonio Aguilar-Palomares, Josué O. Ramírez-Jarquín, and  Fatuel Tecuapetla

<https://doi.org/10.1523/ENEURO.0173-21.2021>

Instituto de Fisiología Celular, Universidad Nacional Autónoma de México, Ciudad de México 04510, México

## Abstract

Striatal activity is necessary to initiate and execute sequences of actions. The main excitatory input to the striatum comes from the cortex. While it is hypothesized that motor and premotor cortico-striatal projections are important to guide striatal activity during the execution of sequences of actions, technical limitations have made this challenging to address. Here, we implemented a task in mice that allows for the study of different moments to execute a serial order sequence consisting of two subsequences of actions. Using this task, we performed electrophysiological recordings in the premotor (M2) and primary motor (M1) cortices, and state-dependent optogenetic inhibitions of their cortico-striatal projections. We show that while both M2 and M1 contain activity modulations related to the execution of self-paced sequences, mainly, the premotor cortico-striatal projections contribute to the proper execution/structuring of these sequences.

*Key words:* action sequences; cortico-striatal; motor cortex; optogenetics; premotor cortex; synapses

## Significance Statement

It is currently hypothesized that synapses from the primary motor (M1) and premotor (M2) cortices that innervate the striatum may guide the proper execution of sequences. Here, we evaluated this hypothesis by training animals to execute self-paced sequences: performing recordings in M2-M1 or manipulating their cortico-striatal projections during the execution of these sequences. We show that both, M2-M1 cortico-striatal projections contribute to sequence initiation, however sequence execution is predominantly influenced by M2. Remarkably the contribution of the cortico-striatal projections from M2 is mainly before the initiation of the sequence working to sustain the structure of the sequences, mainly during the beginning. These findings may have implications for pathologic conditions where the self-paced generation of sequences of actions is impaired.

## Introduction

In everyday life, we continuously move between sequences of motor actions. One of the main proposed drivers involved in the learning and execution of motor sequences are cortico-striatal projections. The study of action sequences in relation to cortico-striatal function has become increasingly important since the discovery

that symptoms in patients with Parkinson's disease and obsessive-compulsive disorder maybe be caused by disruptions to cortico-striatal projections (Graybiel, 1998; Redgrave et al., 2010; Burguière et al., 2013).

The striatum, the primary input to basal ganglia (BG), is a subcortical structure whose activity is necessary to initiate and execute a sequence of actions (Cui et al., 2013;

Received April 17, 2021; accepted August 8, 2021; First published August 31, 2021.

The authors declare no competing financial interests.

Author contributions: A.S.-F. and F.T. designed research; A.S.-F., K.I.R.-A., E.D.-H., A.A.-P., and J.O.R.-J. performed research; A.S.-F., K.I.R.-A., A.K.V.-R., E.D.-H., and A.A.-P. analyzed data; A.S.-F. and F.T. wrote the paper.

Jin et al., 2014; Rothwell et al., 2015; Tecuapetla et al., 2016; Dhawale et al., 2021). Recent evidence suggests that a specific subcircuit within the BG, the indirect pathway, is essential for the transition between subsequences (Geddes et al., 2018; Tecuapetla et al., 2016).

The striatum's main glutamatergic inputs come from the cortex and the thalamus (Wilson, 1989). Several studies suggest that the cortical inputs are essential to execute motor sequences (Tanji and Evarts, 1976; Inase et al., 1996; Martiros et al., 2018; Shima and Tanji, 2000; Fujii and Graybiel, 2005; Shima et al., 2007; Burguière et al., 2013; Smith and Graybiel, 2013; Friedman et al., 2015; Rothwell et al., 2015; Kupferschmidt et al., 2017; Martiros et al., 2018). However, the specific contribution of cortico-striatal projections to the execution of self-paced action sequences remains unclear.

To date, it is known that the supplementary motor area in primates (SMA), which corresponds to the secondary motor cortex (M2) in rodents, is active before starting a sequence of actions (Donoghue and Wise, 1982; Romo and Shultz 1987; Passingham et al., 1988; Shima et al., 2007; Nakayama et al., 2008). SMA activity is important to adapt the behavior in response to contingency changes (block changes; Hikosaka and Isoda, 2010; Siniscalchi et al., 2016). These findings have led to the hypothesis that the premotor cortex guides the striatal activity to initiate and execute action sequences. In rodents, a decrease in the activity of neurons in M2 decreases the probability of alternating between two actions (Rothwell et al., 2015). Strikingly however, studies using cortical lesions suggest that the striatum (BG) can control the execution of a sequence of actions independently from the cortex (Kawai et al., 2015; Dhawale et al., 2021). Therefore, we implemented a self-paced serial order sequence task that allows for probing the contribution of M2 cortico-striatal projections during the initiation, execution, and transition between subsequences of actions. By recording neuronal activity in premotor (M2) and primary motor (M1) cortices and performing time-dependent optogenetic inhibitions of the cortico-striatal projections, we identified specific contributions of the premotor cortico-striatal projections to the execution of self-paced

serial order action sequences. Our results support a model in which the cortico-striatal terminals from M2 guide the appropriate execution of self-paced sequences of actions.

## Materials and Methods

### Animals

The institutional committee of the Cell Physiology Institute, at the National Autonomous University of Mexico, approved all procedures for the care and use of laboratory animals (protocol number FT121-17). This protocol follows the National Norm for Animals' use (NOM-062-ZOO-1999). Male and female mice from two to three months of age at the start of experiments were used for this study. Two genotypes were used: C57BL/6J (The Jackson Laboratory, RRID: [IMSR\\_JAX\\_000664](#)) or Emx1-Cre mice (targeting the Cre recombinase expression in pyramidal cortical neurons), which had been backcrossed into C57BL/6J for at least six generations (Gorski et al., 2002). Emx1-Cre parental line was donated by Professor Rui M. Costa from the Champalimaud Center for the Unknown (RRID: [MGI\\_5141283](#)). All animals were obtained from our breeding colony in our institutional bioterium (the Emx1-Cre line is maintained in heterozygosis). Animals are housed under a 12/12 h light/dark cycle (lights on at 6 A.M.) with *ad libitum* access to food and water before beginning behavioral experiments.

### Training

We used operant conditioning boxes equipped with two retractable levers to implement forced and self-paced serial order sequences in mice (21.6 cm long × 17.8 cm wide × 12.7 cm high; Med-Associates, catalog #MED-307W-D1). One lever was positioned on the left panel (subsequence 1; S1), and the other was located on the front panel (subsequence 2; S2) on the left side of the magazine (Fig. 1B,C). A small sugar pellet, 14 mg (Bio-Serv, catalog #F05684), was delivered as a reward in the magazine. Entries to the magazine were registered with an infrared beam. A second infrared beam was positioned between the magazine and left lever press (Fig. 1B,C) to calculate the latency to start the sequences of actions. Mice were subjected to food restriction throughout training and given enough food after daily training sessions to keep them at 80–85% of their original weight, depending on performance.

For the first exposure to the operant box, animals were placed in the box without levers for 30 min. A total of 30 pellets were delivered individually at random intervals (on average every 60 s). Over the next 3 d, the animals were presented with lever 1 or lever 2 and received a reward each time they pressed the lever. After eight rewards, lever 1 was retracted, and lever 2 was presented. The session finished once the animal got 16 pellets, or 30 min had passed. Afterward, the training schedule changed to 3 d at a fixed ratio eight (FR8) schedule on each lever, whereby animals had to accumulate eight lever presses to receive a reward and retract the lever, followed by a second lever presentation, which also required 8 presses to

This work was supported by the Ciencia Basica Consejo Nacional de Ciencia y Tecnología (CONACyT) Grant 220412; Fronteras de la Ciencia CONACyT Grants 2022 and 154039; Dirección General de Asuntos del Personal Académico - Programa de Apoyo a Proyectos de Investigación e Innovación Tecnológica (DGAPA-PAPIIT)-Universidad Nacional Autónoma de México (UNAM) Grants IA200815, IN226517, and IN203420; and the Catedra Marcos Moshinsky 2019 (F.T.). A.S.-F. is a doctoral student from the Programa de Doctorado en Ciencias Biomédicas, UNAM and has received the CONACyT Fellowship 597738.

Acknowledgements: We thank Professor Rui Costa for the Emx1-cre mice, Dr. E. Galarraga for electrophysiology *ex vivo* support, Dr. Y. Ramiro-Cortes for imaging support, and Dr. Gabriela J. Martins and Dr. Anna Hobbiss for proofreading the English of this manuscript.

Correspondence should be addressed to Fatuel Tecuapetla at [fatuel@ifc.unam.mx](mailto:fatuel@ifc.unam.mx).

<https://doi.org/10.1523/ENEURO.0173-21.2021>

Copyright © 2021 Sánchez-Fuentes et al.

This is an open-access article distributed under the terms of the Creative Commons Attribution 4.0 International license, which permits unrestricted use, distribution and reproduction in any medium provided that the original work is properly attributed.

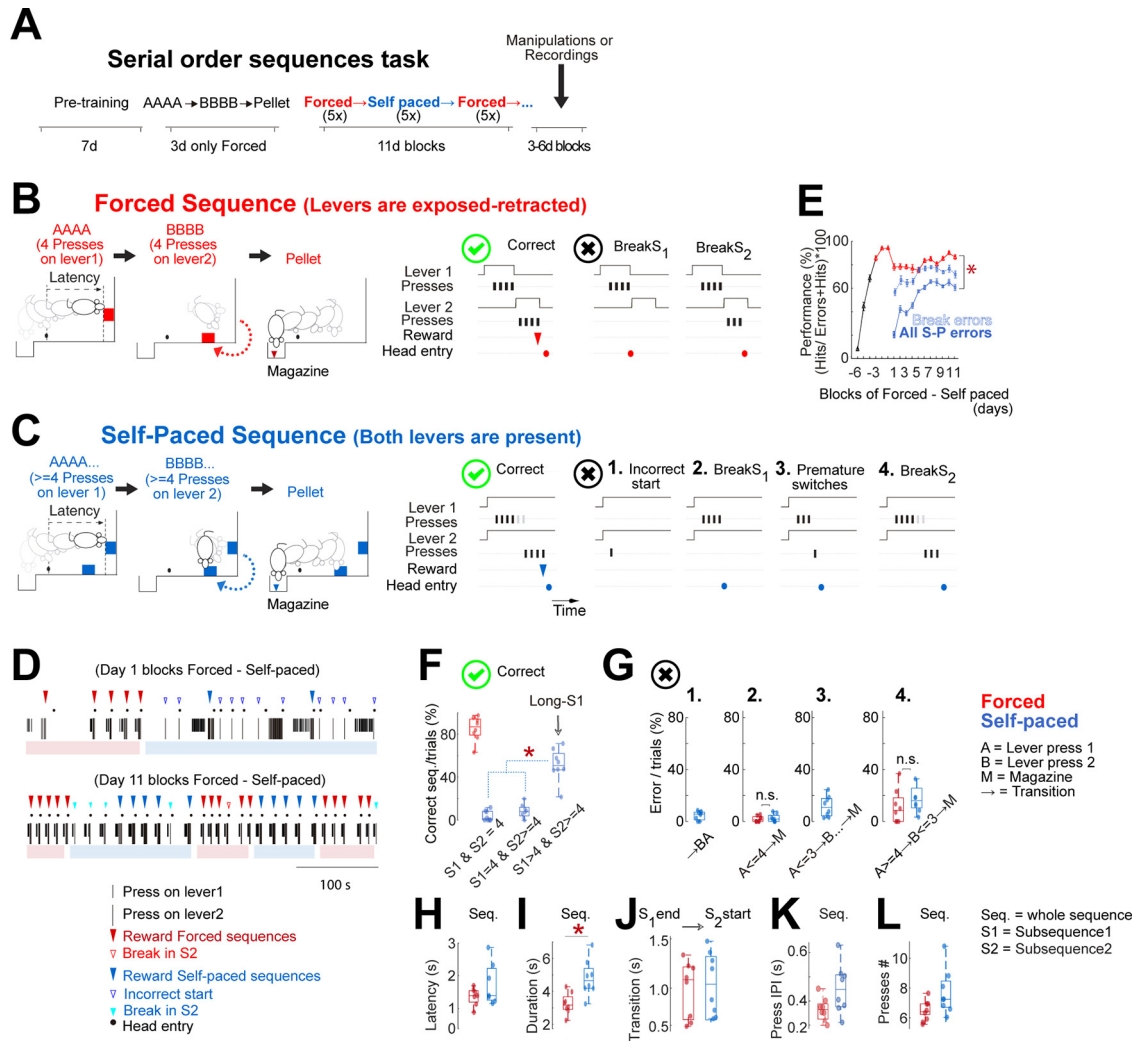


**Figure 1.** Mice learn to execute serial order sequences of lever press. **A**, Timeline of training days. After 7 d of pretraining (see Materials and Methods), animals enter a phase of forced sequences (AAAA→BBBB→pellet). After 3 d, animals started training on blocks of forced and self-paced sequences, switching blocks once five correct trials are achieved per block. **B**, left, Diagrams of the sequential pressing on lever 1 (AAAA = 4 presses) → lever 2 (BBBB = 4 presses) delivering a reward in the magazine (pellet) in forced sequences, where levers are presented individually. Right panels, Correct forced sequence depicted with a green symbol and the two different categories of errors that mice executed in forced sequences. **C**, left, Diagrams of the sequential pressing on lever 1 (AAAA... >= 4 presses) → lever 2 (BBBB... >= 4 presses) delivering a reward in the magazine (pellet) in self-paced sequences, where levers are presented together. Right panels, Example of a correct sequence depicted with a green symbol and the four categories of errors that mice executed while performing self-paced sequences. **D**, Example of the sequences of one animal's presses during the first day (early in training) and eleventh day (late in training) during sessions of blocks of forced-self-paced sequences. Note how the self-paced sequences become very stereotyped late in training [the blocks are indicated by light red (forced) or light blue (self-paced) at the bottom of each panel]. **E**, Percentage of correct sequences [correct/(errors + correct)]. Note that day 1 in the x-axis means the first day in which animals were required to perform blocks of forced and self-paced sequences as explained in **A-C**. However, the requirement of forced sequences (AAAA→BBBB→pellets) was present 3 d before. All curves show mean ± SEM WT (n = 8). **F**, The correct forced sequences were of one type (S1 = 4→S2 = 4) but of several types for self-paced sequences, dominated by Long-S1 sequences (S > 4→S2 >= 4). **G**, The different categories of errors that mice executed while performing forced or self-paced sequences late in training. **H-L**, Mean duration, transition, interpress intervals, number of presses from WT animals (n = 8) measured late in training; \*p < 0.05, specific p values and statistical test specified in the text and Table 1. Extended Data Figure 1-1 includes the latency, transition time, IPI along with training, and a comparison of the proportion of the different errors early and late in training. n.s. = p > 0.05.

receive the reward and retract the second lever (pretraining). The session finished when mice reached 30 rewards (15 on lever 1, 15 on lever 2) or 30 min had passed. If the animals checked the magazine before reaching eight

continuous lever presses, a time out (10 s) was presented. We used 3 d in FR8 since in previous studies have seen this induces animals to press in bouts of around four presses (Tecuapetla et al., 2016). Next, animals were

trained to do forced serial order sequences (3 d). Here, animals were presented with a lever 1; they had to do four continuous lever presses for the lever to be retracted, followed by extension of a second lever (lever 2). Animals had to do four continuous lever presses on lever 2 for it to be retracted, and a reward was delivered into the magazine (Fig. 1B). If the animals executed fewer than four lever presses on lever 1 or lever 2 by visiting the magazine, a time out (10 s) was presented. The session finished when mice got 30 rewards, or 30 min had passed. After these 3 d of forced sequences, the animals entered the last stage of training: blocks of forced–self-paced sequence sessions. These sessions began with a block of forced trials, switching to a block of self-paced trials in the same session. The switch between blocks was conditioned by achieving five consecutive correct sequences. For the self-paced sequences, the animals were presented with the two levers at the same time. They had to do at least four presses on lever 1 followed by at least four presses on lever 2, to obtain a reward in the magazine. Unlike in forced blocks, in self-paced blocks the animals decided when to execute the transition between the subsequences of presses from lever 1 to lever 2 (Fig. 1C). Upon finishing a self-paced block, both levers are retracted for 3 s for an intertrial interval before starting a new forced block. If the animals executed fewer than four presses on lever 1 or lever 2 by visiting the magazine, a time out (10 s) was presented. The session finished once the animals received 70 rewards (35 forced and 35 self-paced rewards) or 30 min had passed. The block sessions continued for 11–13 d until a stable performance was reached; see Fig. 1E). All timestamps were recorded with a resolution of 10 ms with the Med-PC IV software suite (Med-Associates).

### Single-unit recording and antidromic photo-identification

To record the cortical activity, either a fixed or movable 16-electrode array [tungsten (35  $\mu\text{m}$ ; Innovative Neurophysiology) was implanted]. The neurons' spikes were sorted online (Central software, Blackrock Microsystems), and clear waveforms with a signal-to-noise ratio  $>3:1$  were used for further analysis using offline-sorting (Offline Sorter, Plexon Inc.). To define whether a recorded unit projected to the striatum, we used *in vivo* antidromic photo-identification (Lima et al., 2009). In short, we injected Chr2 (UPENN-vector core catalog #AV-1-20298P) in the cortex of interest of Emx1-Cre animals. A movable electrode array was implanted 200  $\mu\text{m}$  above the Chr2 expression site during the same surgery, and an optic fiber (Thorlabs catalog #CFLC230-10, FT200EMT) was implanted into the striatum (ipsilateral to injection). Using the electrode array, we could record activity of cortical neurons. At the end of the behavior session, we used a light stimulation (2 mW, 473 nm, 10 Hz, 1 s, 10-ms pulses; Laserglow) delivered by the optic fiber while recording neuronal activity. This allowed us to verify whether the recorded neuron was antidromically photo-activated (Extended Data Fig. 3-2). The movable array allowed us to search for responding cells in at least five sessions per animal, advancing the array 100  $\mu\text{m}$  24 h before the recording. Only units that responded to the light (i.e.,

presented a correlation of  $>0.9$  between the behavioral spike and the antidromic spike and presented a latency to light  $<10$  ms) were considered.

### Per-trial rescaling of neural activity

In both sequence types, forced and self-paced, each sequence had a slightly different durations and could not be directly averaged. To mitigate this, we employed a time rescaling procedure (Kobak et al., 2016), to evaluate each recorded unit's overall response pattern. Thus, we performed a rescaling of trials with at least four presses in each sequence, defining the following alignment events: first, second, penultimate, and last press of subsequence 1 and subsequence 2. Spike trains were transformed to instantaneous firing rate by applying a Gaussian convolution ( $\sigma$  25 ms) at 100 Hz. The activity was rescaled through linear interpolation to the average interpress interval and inter sequence interval of all recorded animals' sessions.

### Analysis of the electrophysiological recordings *in vivo*

Once a putative unit was isolated (through online and off-line sorting), the spikes' timestamps were aligned to the first lever press in the sequences of actions using custom-developed scripts in MATLAB (MathWorks).

Z score test: to determine differences between the z score activity from M2 versus M1, we averaged the z score activity in the same time window from the two indicated cells and calculated the difference in terms of z score with the following equation:

$$Z_{\text{difference}} = \frac{Z_1 - Z_2}{\sqrt{\left(\frac{1}{N_1 - 3}\right) + \left(\frac{1}{N_2 + 3}\right)}}$$

where  $Z_1$  is the average normalized activity of the M2 units and  $Z_2$  for the M1;  $N_1$  is the sample of units from M2, and  $N_2$  the sample of units from M1 (Fig. 2J; Extended Data Fig. 2-1H). The results were compared in a normal distribution table to determine the corresponding  $p$  value (Chen and Popovich, 2011).

### Regression analysis of the neuronal activity and behavior

We made linear regression analysis to ask whether the firing rate in each bin of time was correlated with parameters of the task. For this purpose, we first aligned the spikes to each epoch (first, second, penultimate, and last lever press for each sequence) and took 5 s before and 5 s after each epoch. Spike trains were transformed to instantaneous firing rate as described above. We calculated the spike frequency using a 200-ms time window with 10-ms steps. We separated the trials and sorted them by the number of lever presses in the sequences (2,4,6, up to 16, grouped by every increment), for the sequence and transition duration (sorted by duration in descending manner, seven categories), for latency (grouped every one second, starting with 0.5 s.). Then we made a regression analysis with permutation test in two manners. For the first, we used a bin of time of 200 ms with a sliding window of

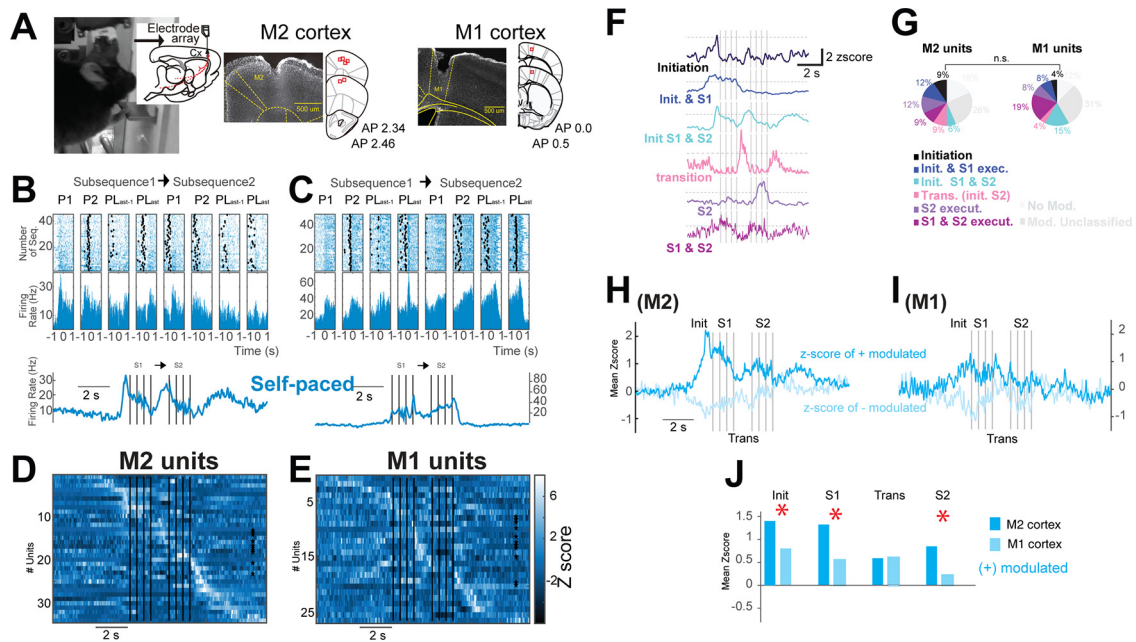


**Figure 2.** Activity modulation in premotor and motor cortical neurons during the execution of self-paced sequences of actions. **A**, Image of a mouse while pressing one of the levers and photomicrographs of coronal sections of M2 (middle) or M1 cortex (right), illustrating the cannula/electrode array's tracks in the recorded sites. **B**, **C**, Raster plots and perievent histogram from an M2 or an M1 unit, respectively, aligned to the first (P1), second (P2), penultimate (PLast-1), and last lever press (PLast) of S1 and S2 for self-paced sequences. Bottom panels, Mean firing rate from the upper panels. **D**, **E**, Z score of individual units. **F**, Representative firing of different cells presented as z score, illustrating the different categories of modulation during the execution of the sequences Init & S1 execu = Initiation and S1 execution; Init. S1 & S2 = Initiation of S1 and S2; Trans.(init. S2) = Transition or initiation S2; S2 execut. = S2 execution; S1 & S2 execut. = S1 and S2 execution. **G**, % of cells related to each category in **F**. **H**, **I**, Mean z score from the units recorded that presented significant modulation 1 s before the initiation of the sequence from M2 or M1. **J**, Comparison of the mean z score from **H**, **I**, M2 (dark blue) versus M1 (light blue) for positively modulated units; \* $p < 0.05$ , z score test. Init. = initiation, S1 = subsequence 1, Trans = transition, and S2 = subsequence 2. Extended Data Figure 2-1 includes the activity modulation in premotor and motor cortical neurons during the execution of forced sequences of actions. n.s. =  $p > 0.05$ .

10ms and ask whether the variable of interest was correlated with the firing rate (Fig. 3A; Extended Data Fig. 3-1B). For the second regressions analysis, we used specific windows of time: (1) mean firing rate 1 s before the start of the sequence; (2) mean of firing rate during the sequence; (3, 4, and 5) average of firing rate during S1, firing rate during transition or firing rate during S2 (Fig. 3B). To resolve statistically whether the regression's  $p$  value was significant, we ran 1000 permutations and divided the sum of times that the  $p$  value  $> p$  value initial between the number of permutations. Only regressions with  $\beta$  coefficient different from zero ( $p < 0.05$  and  $R > 0.6$ ) were accepted.

### ROC curve analyses and permutations

To determine the percentage of modulated units along time in each epoch, we performed a ROC curve analysis to ask whether the spike frequency in each time bin was different from baseline time. We first aligned the spikes to each epoch (e.g., first press) using 4 s before and 5 s after each epoch. We calculated the spike frequency using a 200-ms time window. We used a baseline from -4.5 to -4 s before the first press in the sequences. We compared the spike frequency in each bin of time against the baseline, using a sliding window of 10 ms. To resolve

statistically whether the area under the curve (AUROC) was significant, we ran 1000 permutations and divided the sum of AUROC values that fall in either  $>0.5$  or  $<0.5$ , by the number of permutations. The AUROC value was significant if the outcome was  $p < 0.05$ . Furthermore, in each epoch, we obtained a binary matrix comparing each bin to baseline. This binary matrix was used to find the number of units modulated in each time bin. For the linear regression, to resolve statistically whether the regression's  $p$  value was significant, we ran 1000 permutations and divided the sum of times that the  $p$  value  $> p$  value initial between the number of permutations.

### Stereotaxic opsin injection and fiber implantation

For surgeries, animals were anesthetized using a mix of oxygen (1 l/min) and 1% isoflurane (1–2% for interventional procedures). For the optogenetic experiments: after anesthesia, each animal was bilaterally injected using glass pipettes with 500 nl of viral stock solution [either rAAV5-EF1a-DIO-eArch3.0-EYFP (Vector core, University of North Carolina), or AAV1.EF1a.DIO.eYFP.WPRE; AAV1.EF1a.DIO.hChR2(H134R)-eYFP.WPRE titer  $> 1 \times 10^{12}$  (Vector core UPENN University Pennsylvania catalog #AV-127056)] by pressure into either the M2 or M1 or lateral striatum (LS), coordinates from bregma, M2: AP

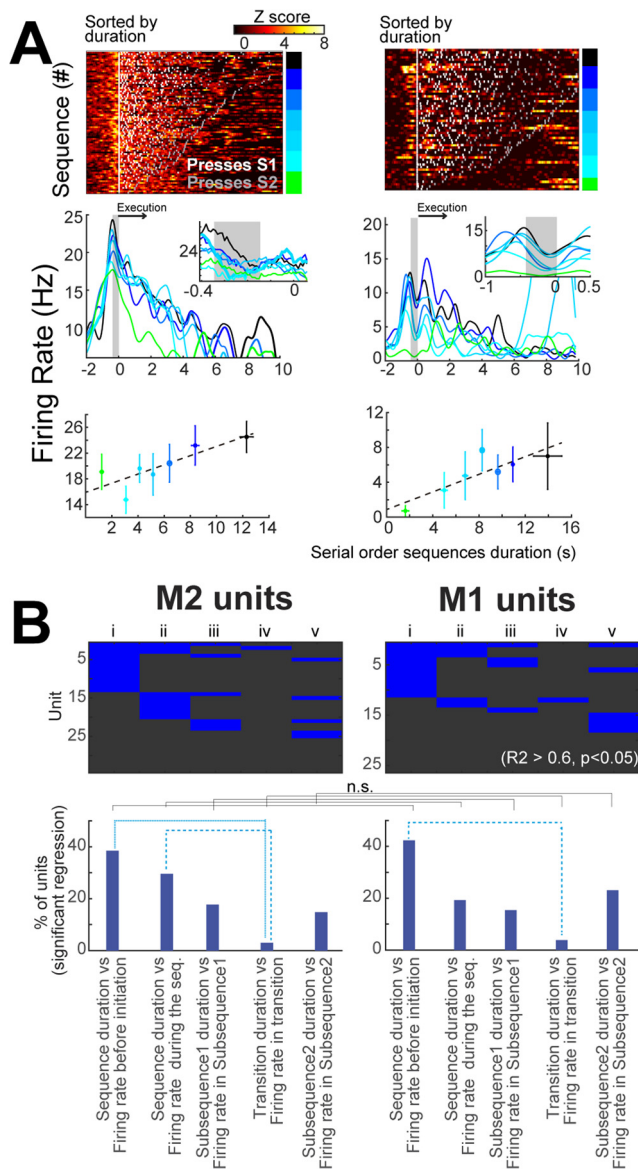


**Figure 3.** Both M2 and M1 contain units encoding the temporality of the self-paced sequences of actions. **A**, top panels, Examples of two units recorded in M2. In each example, each line is a self-paced sequence depicting the neuronal activity (in z score, black to yellow) and lever press (white points subsequence 1, gray points subsequence 2). The color bar to the right of each plot shows the grouped categories plotted in the middle and bottom panels. Middle row panels, Mean firing rate from each category presented in the upper row. Bottom row, Regression fits from the time bin depicted in gray in the middle row panels. **B**, top row panels, Significant regression analysis per unit; columns i, between the firing rate (FR) 1 s before the start of the sequences (Seq) versus the duration of the sequences; columns ii, FR during the sequences versus duration of sequences; columns iii, FR in the subsequence 1 (S1) versus the duration of S1; columns vi, FR during the transition versus the transition time; and columns v, FR during the subsequence 2 (S2) versus the S2 duration. Bottom panels, The proportion of units that presented significant regression ( $R^2 > 0.6$  and  $p < 0.05$ ). The dashed lines depict comparisons with  $\chi^2$  test. Corrections for multiple comparison was considered (see Materials and Methods). Extended Data Figure 3-1 shows the

*continued*

recorded units in M2 or M1 encoding the temporality of the forced sequences of actions. Extended Data Figure 3-2 shows the confirmation of the M2-M1 projections into the LS and linear regressions between the activity and the temporal parameters of the execution of sequences from the photo-identified M2 or M1 cortico-striatal neurons. n.s. =  $p > 0.05$ .

2.34 mm, ML 1.25 mm, DV 0.60–0.70 mm. M1: AP 0.5 mm, ML 1.60 mm, DV 0.60–0.70 mm. LS: AP 0.50 mm, ML 2.50 mm, DV 2.40 mm below the brain’s surface. After the injections were done (23 nl every 5 s; Nanoject II, Drummond Scientific), we waited 15 min to allow time for virus to spread, and a fiber-optic (300  $\mu\text{m}$ ; NA 0.37) was implanted into each hemisphere of the striatum. The optical fibers were fixed to the skull using acrylic cement (Lang Dental Manufacturing Co, Inc).

**Retrobead injections**

For the retrograde labeling experiments, 300 nl of retrobeads (Lumafuor) were injected into the LS. Coronal sections (50  $\mu\text{m}$ ) were obtained to determine the total number of cells labeled in the M2 or M1. The quantification was done in one slice every 300  $\mu\text{m}$  covering these regions.

**Retro-Cre injections**

Similarly, to the retrobead injections, 300 nl of mCherry-Retro-Cre (Addgene catalog #55632-AAVrg, RRID: [Addgene\\_55632](#)) AAV were injected into the LS, and 300 nl of DIO-eYFP were injected into the M2 cortex of Emx1-Cre. Coronal striatal sections of 50  $\mu\text{m}$  were obtained to determine the axons crossing by the dorsomedial or the dorsolateral striatum.

**Cortico-striatal fibers quantification**

The axonal quantification protocol was as previously reported (Díaz-Hernández et al., 2018). In short, we extracted the brains and sectioned the striatum (50- $\mu\text{m}$  coronal sections). Z stacks at 63 $\times$  magnification were acquired (192  $\times$  192  $\times$  10  $\mu\text{m}$ ; 1- $\mu\text{m}$  interslice) from a random quadrant; using a randomly positioned grid covering either the dorsolateral or the dorsomedial striatum (ZEN lite software, Zeiss, LSM 710). These Z stacks were imported into ImageJ; then, a maximum projection image was used to apply a filter (Hessian filter), allowing the quantification of fibers as defined by the number of fibers crossing a randomly generated line spaced  $\sim 20 \mu\text{m}$ .

**Cortical microstimulation of forelimb region in the M1**

Micro-stimulation experiments were performed to identify the M1’s coordinates corresponding to the contralateral forelimb region. The animal was placed in the stereotaxic apparatus under anesthesia (ketamine 0.15 mg/g mouse + xylazine 0.01 mg/g mouse). Access to motor cortex was achieved by trepanning a window of at least 1 mm in diameter around the center point (AP +1, ML 1). Electrical stimulation was performed using a 300- $\mu\text{m}$  concentric bipolar electrode on the dura’s surface with 15 square pulses of 200  $\mu\text{s}$  at a frequency of 200 Hz using a stimulator device

(DS2, Digimiter). With the administration of voltage pulses, we looked for contralateral forepaw movement and corroborated this using a camera. This stimulation was performed on a grid every 100  $\mu\text{m}$  in the AP and ML direction. The coordinates where the stimulation resulted in movement of the contralateral brachial biceps were taken to implant the recording electrode (mouse1: AP 0.5, ML 1.5; mouse 2, AP 0.0, ML 1.5).

### Temporally defined optogenetic striatal inhibition *in vivo*

Light was delivered via 300 micrometer-diameter implantable fibers (Doric lenses) coupled to a single longitudinal mode laser (MSL-FN-556, CNI lasers; 556 nm). For the optogenetic inhibition experiments, a free launching system controlled by an AOM (AAoptoelectronics) and fast speed shutter (Thorlabs catalog #SH5, SC10) triggered by TTL output from the MED-PC behavioral box was used to deliver the light. Power at the fiber tip was verified for every experiment using a power meter (Thorlabs catalog #PM130D). The power was adjusted to be 20 mW at the tip of the fiber for the green light. To define the time point for the optogenetic inhibition of the cortico-striatal projections before the initiation of sequences, we took advantage of the fact that animals developed stereotypical sequences. Thus, when the animal moved from the magazine to the first lever (left lever), the infrared beam was broken, sending the timestamp to trigger the light on and allowing the quantification of the latency to initiate the sequences of actions (Figs. 1B,C, 4G; Extended Data Fig. 4-1C,I,O). To define the time point for the light manipulations during the sequences' execution, we used the timestamp of the first lever press in the sequences (Fig. 5A). To define the time point for the light manipulations during the transition between forced subsequences, we used the timestamp of the penultimate lever press of subsequence 1. In self-paced sequences, we quantified the mean of lever presses to define a penultimate lever press (although we confirmed that it was two presses before the last of S1 in this case; see Fig. 6B). During the session of optogenetic inhibition, there were control (light off) trials and stimulation trials. The stimulation trials were randomly presented throughout the session (50% of total trials).

### Behavioral quantification during optogenetic inhibitions

The percentage of correct sequences of actions was quantified. A correct sequence was defined as the sequence with at least four presses on the first lever followed by at least four lever presses on the second lever. We also calculated the proportion of incorrect sequences (errors; Fig. 1G), by dividing the number of incorrect sequences by the total number of stimulation trials (on trials) or control light trials (off trials). Latency to initiate was calculated as the time between crossing the infrared beam out of the magazine and the first lever press in the sequences. The duration of a sequence was the time from the first press of subsequence 1 to the last press of subsequence 2. The transition between sequences was the time from the last press in subsequence 1 to the first

press in subsequence 2. All animals were video recorded during the optogenetic manipulations. This allowed us to verify that all animals used both forepaws to execute the presses.

### *Ex vivo* whole-cell recordings

To express ChR2 in the M2 cortico-striatal projections, we injected 300 nanoliters of ChR2 into M2 ( $n=4$  mice). After 8–16 d, the animals were deeply anesthetized and transcardially perfused to obtain striatal slices as described in Díaz-Hernández et al. (2018). Postsynaptic currents in whole-cell configuration were evoked by pulses of blue light (1 ms), with a pair of cells (one dMSN and one iMSN) recorded per slice. The recordings were acquired as described in Díaz-Hernández et al. (2018).

### Experimental design and statistical analysis

Significance was determined by  $p < 0.05$ . For the proportions, paired or between groups, the  $\chi^2$  test, the Wilcoxon test, or the Mann–Whitney  $U$  test was used, as appropriate. For comparisons along sessions, a non-parametric Friedman statistical test was used. When multiple comparisons were employed, a Benjamini–Hochberg correction was used to adjust the  $p$  value (Fig. 3B; Extended Data Figs. 3-1A, 3-2G). All statistical analyses were performed using GraphPad, R [R core Team (2013)] and MATLAB. Additionally, for the optogenetic manipulations experiments, we use estimation statistics based on confidence intervals (CIs) as described in Ho et al. (2019) and Manouze et al. (2019). The effect sizes and CIs are reported as: effect size [CI width lower bound; upper bound]. Five thousand bootstrap samples were taken, and the  $p$  value(s) reported are the likelihood(s) of observing the effect size(s), if the null hypothesis of zero difference is true. To account for multiple comparisons at each inhibition protocol, we considered a false discovery rate (FDR)-adjusted  $p$  value ( $q$  value)  $< 0.10$ , two-sided, as significant (Storey, 2002).

### Data and software availability

All data and MATLAB scripts will be available on request to the lead or corresponding authors.

## Results

To identify the premotor cortico-striatal contribution to serial order sequence execution, we developed a behavioral task in mice allowing us to perform two types of experiments. Mice were trained to execute two subsequences of lever presses on two levers in serial order (Fig. 1). For the first experiment, we aimed to identify whether neuronal activity in M2 or M1 is modulated during the task's serial order sequences. We performed *in vivo* electrophysiological recordings in M2 or M1 to measure neuronal activity while animals executed these lever press sequences (Figs. 2, 3). For the second experiment, we aimed to identify whether the projections from these cortical regions contribute to the sequences' execution, by optogenetically inhibiting the cortico-striatal projections either before or during the sequences' execution, or during the transition between the two subsequences (Figs. 4-6).

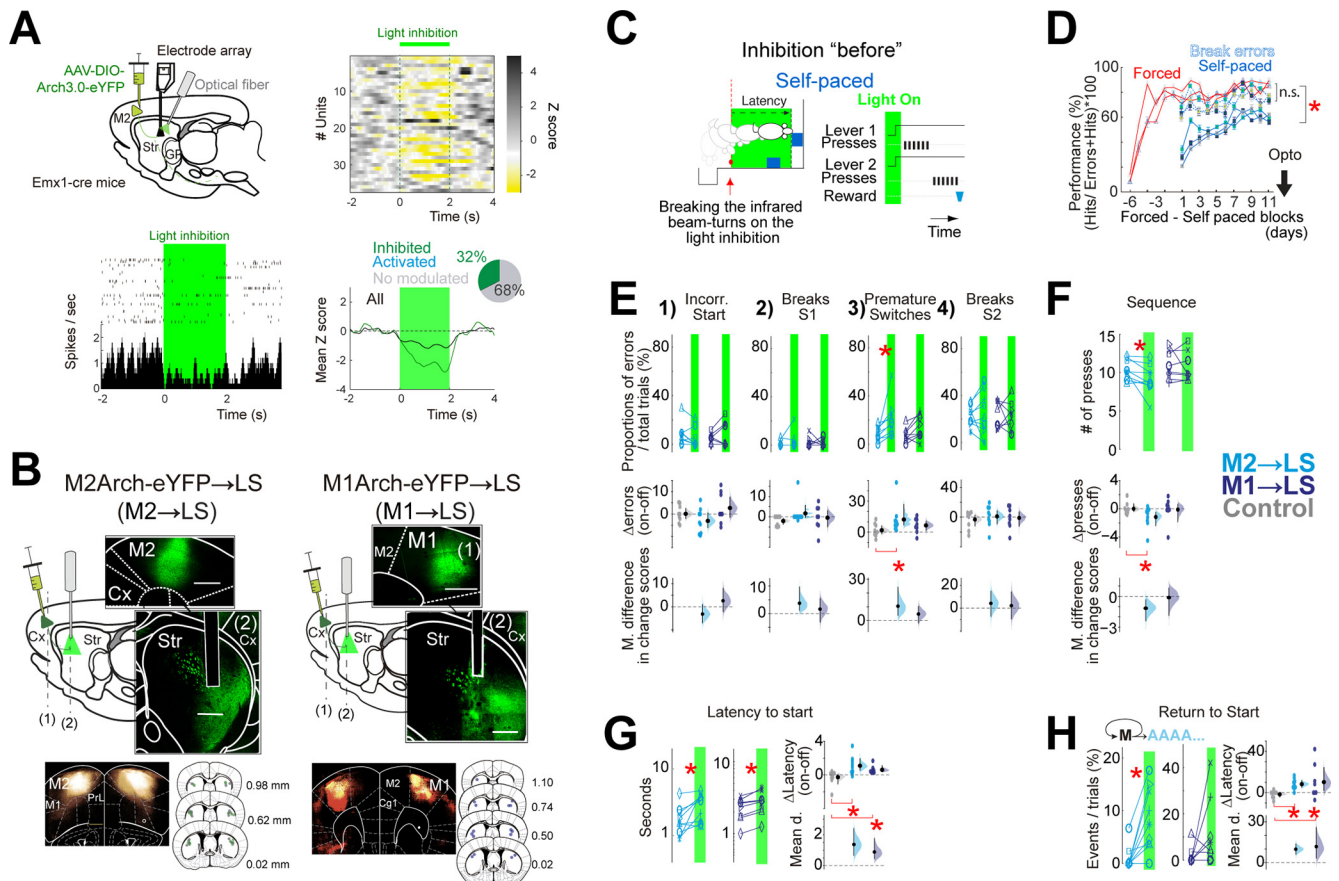


**Figure 4.** The inhibition of the premotor and primary motor cortico-striatal projections before sequence initiation, but only the premotor disrupts the execution. **A**, top left, Diagram illustrates the injection site of Arch3.0-eYFP and the optrode (electrode array+ fiber optic) implantation into the LS. Top right, Plot depicting the activity of several units recorded in the striatum (z score) aligned to the inhibition of the M2 cortico-striatal projections into the LS (green line above). Bottom left, representative per-event time histogram and raster plot of a striatal unit's activity aligned to the inhibition of the M2 cortico-striatal projections (green shadow). Bottom right, Mean z score for the units that decreased their activity (green) or for all units recorded (black) during the inhibition. Inset, Pie chart showing the proportion of modulated and non-modulated units (comparing baseline time vs light). **B**, top panels, Sagittal diagrams and cortical photomicrographs of the injection of Arch3.0-eYFP into either M2 ( $n = 9$ ) or M1 ( $n = 8$ ) cortices and optical fibers implantation into the LS (Str). Scale bar: 500  $\mu$ m. Bottom panels, Photomicrograph showing the average of Arch3.0-eYFP expression of the corresponding groups. Coronal diagrams representing the position of the optical fiber's tips into the LS (green dots: Arch3.0-eYFP; gray dots: eYFP). **C**, Scheme of the inhibition protocol before the initiation of the sequences. The light inhibition (2 s) is triggered by breaking the infrared beam positioned outside of the magazine, when coming to the lever (dashed red lines on the schemes). **D**, Percentage of correct sequences [correct/(errors + correct)] throughout training. **E**, upper panels 1–4, Quantification per animal in off versus on trials of the proportion of each category of error. **F**, Effect of the inhibition on the number of lever press per sequence. **G**, Effect of the inhibition of the cortico-striatal projections on the latency to initiate self-paced sequences. **H**, Effect of the inhibition of the cortico-striatal projections on the proportions of times per block that animals returned to the magazine after having crossed the infrared sensor outside of the magazine (which set the timestamp to trigger the light inhibition; see Movie 3). On the paired plots, each line depicts the mean effect per animal during trials of optogenetic inhibition (on; green shadow) versus trials without optogenetic inhibition (off; no shadow) from the same session. In panels **E–H**,  $\Delta$  on-off panels are obtained from the mean difference per animal in the on-off trials, adding the control group in gray. The mean difference in change score panels (mean d.) are obtained between the experimental groups and the control group (see Materials and Methods). Paired plots, two-sided permutation  $t$  test; panels  $\Delta$  on-off, Arch animals versus control eYFP animals, unpaired two-sided permutation  $t$  test;  $*p < 0.05$ . The exact  $p$  values are described in the text and Table 1. Extended Data Figure 4-1 shows the effects of the inhibition of the lateral striatal neurons during the initiation and execution of the action sequences. Extended Data Figure 4-2 shows the M2/M1 retrogradely labeled cells from the LS, the thalamus, and the pons. Extended Data Figure 4-3 shows that the premotor cortico-striatal projections innervate the direct pathway with a stronger synaptic weight than the indirect pathway. n.s. =  $p > 0.05$ .

### Mice can learn to execute serial order sequences of lever presses

To investigate the contribution of cortico-striatal synapses to the structuring and execution of self-paced serial order sequences, we trained mice in a serial order task to

execute two subsequences of lever presses (Fig. 1A). The execution of a correct serial order sequence was achieved when animals performed at least four presses on a lever 1 (subsequence 1; S1) followed by four presses on lever 2 (subsequence 2; S2), which lead to the delivery of a

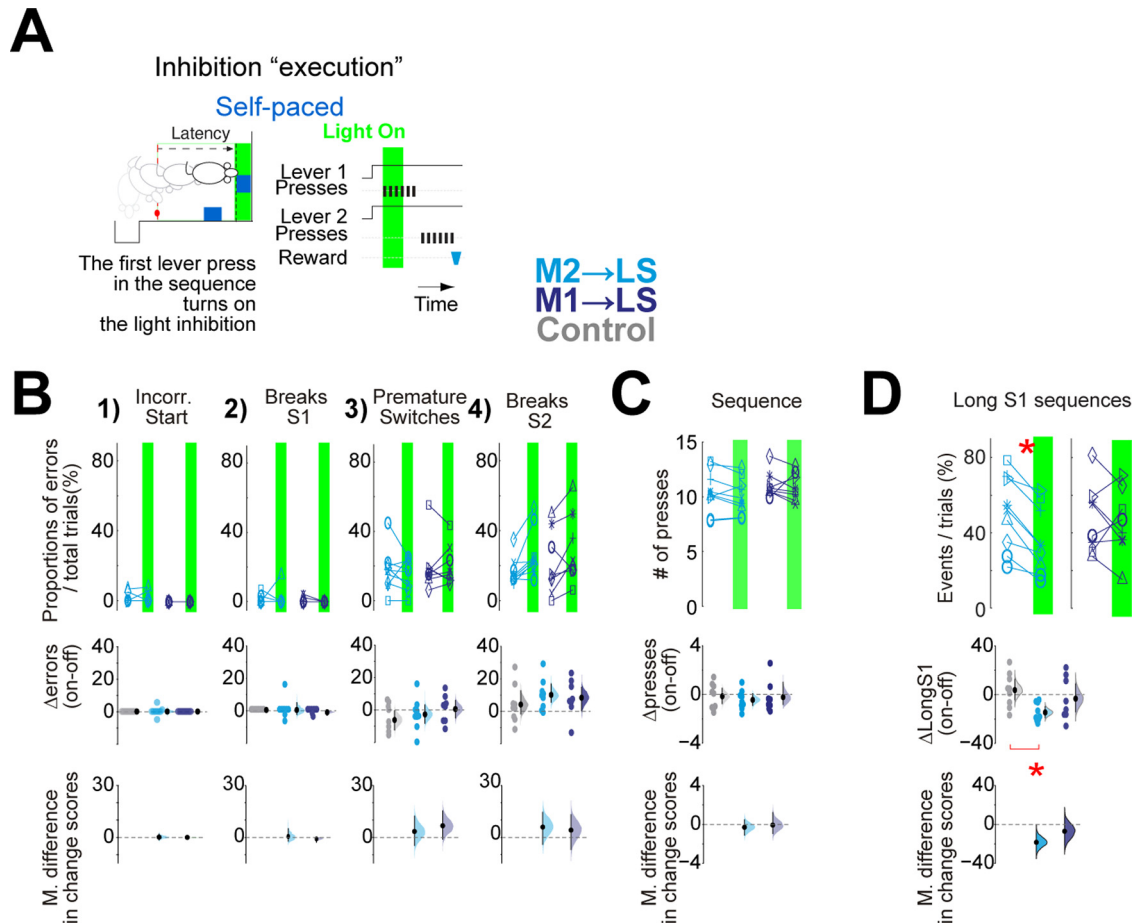


**Figure 5.** The inhibition of premotor cortico-striatal projections at the start of the execution decreased Long-S1 self-paced sequences. **A**, Scheme of the inhibition execution protocol. Light inhibition was triggered by the first press in the sequences. The green shadow depicts 2 s of continuous light inhibition. **B**, upper panels 1–4, Quantification per animal in off versus on trials of the proportion of each category of error. **C**, Effect of the inhibition on the number of lever presses per sequence. **D**, As in **B**, **C** evaluating the proportion of animals performing Long-S1 sequences  $S1 > 4 \rightarrow S2 \geq 4$ . On the paired plots, each line depicts the mean effect per animal during trials of optogenetic inhibition (on; green shadow) versus trials without optogenetic inhibition (off; no shadow) from the same session. In panels **B–D**,  $\Delta$  on-off panels are obtained from the mean difference per animal in the on-off trials, adding the control group in gray. The mean difference in change score panels (mean d.) are obtained between the experimental groups and the control group (see Materials and Methods). Paired plots, two-sided permutation  $t$  test; panels  $\Delta$  on-off, Arch animals versus control eYFP animals, unpaired two-sided permutation  $t$  test; \* $p < 0.05$ . The exact  $p$  values are described in the text and Table 1.

reward in the magazine (pellet). To execute self-paced sequences, we first trained animals to execute forced sequences (forced: only one of the two levers was exposed at any point, signaling the animals when to press; Fig. 1B). Later in training, blocks of forced and self-paced serial order sequences were intercalated (self-paced: both levers remained exposed so that animals decided when to press and transition between subsequences; Fig. 1C). The requirement of intercalated blocks was necessary as animals' performance dropped when they were required to perform only self-paced sequences (tested in a group of eight animals: data not shown). The main difference between a forced and a self-paced serial order sequence was that in the former, completing four presses on lever 1 retracted it and exposed lever 2; if four presses were executed on lever 2, it was also retracted, followed by the delivery of a pellet in the magazine (Movie 1). On the other

hand, the execution of a correct self-paced sequence also required at least four presses on each lever, but in this case, both levers remained exposed throughout the self-paced trials (Movie 2).

A session containing both different kinds of sequences is identified in the figures as blocks of “forced–self-paced” sessions. During one of these sessions, the animals were required to achieve correct blocks of five forced and five self-paced sequences consecutively for 30 min. Figure 1D shows an example animal during the first (early) and the eleventh (late) day (rewards are labeled with filled red triangles for forced and in blue for self-paced). After 21 d of training, and 9 d performing blocks forced–self-paced sessions, animals showed a stable performance of correct sequences, demonstrated by the fact that performance no longer changed from sessions 9 to 11 [performance forced,  $\chi^2(2) = 2.51$ ,  $p = 0.30$ , performance self-paced,  $\chi^2(2) = 1.0$ ,

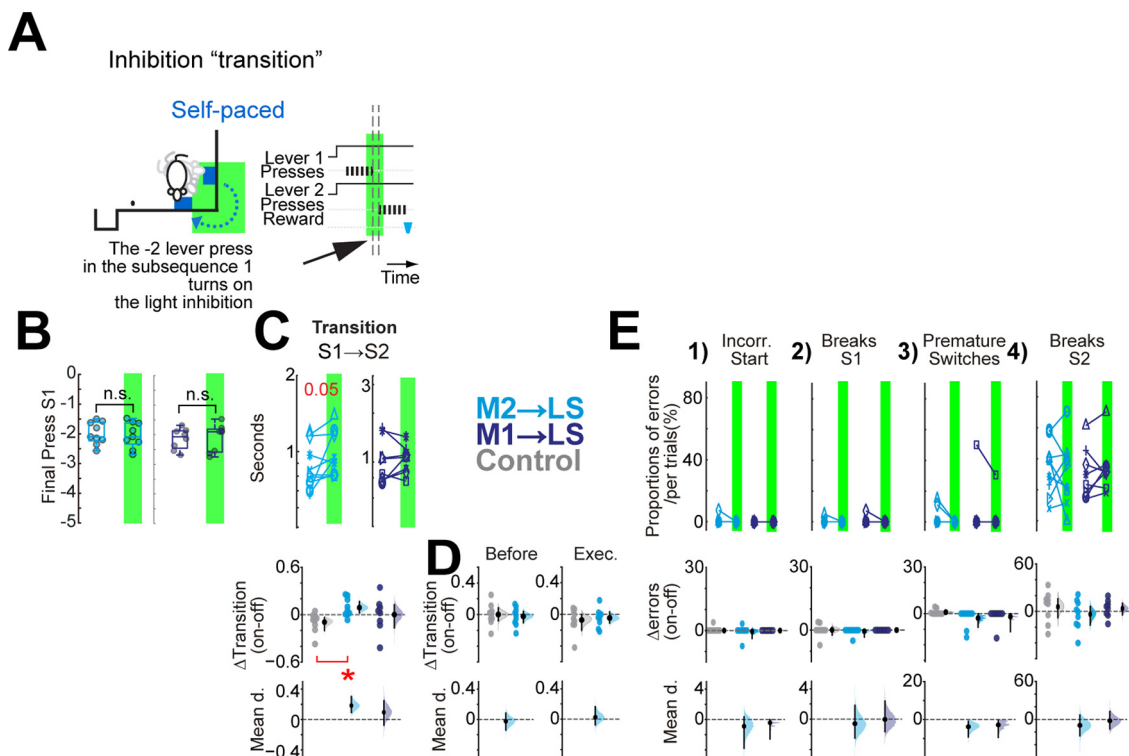
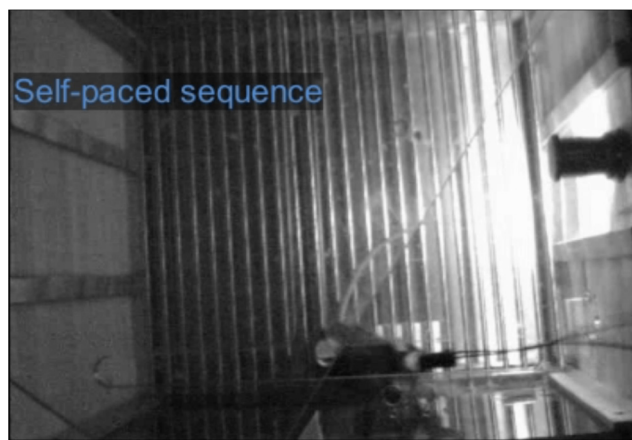


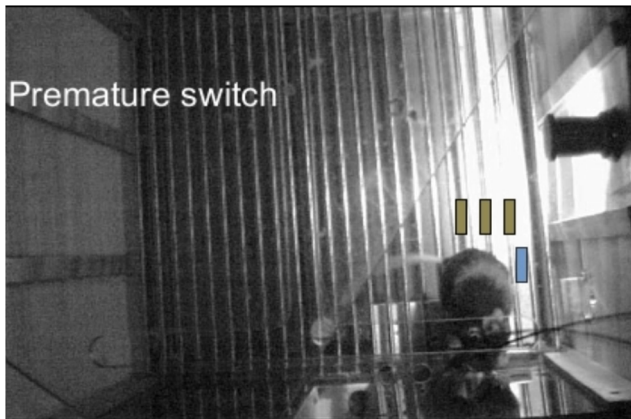
**Figure 6.** Inhibition of premotor but not primary motor cortico-striatal projections at the moment of the transition increases the transition time inside self-paced sequences. **A**, Scheme of the inhibition protocol transition in self-paced sequences. The light inhibition was triggered by the press before the penultimate press of the subsequence 1. The dashed and black arrows denote the period of the transition. **B**, Estimation of the press that delivered the timestamp for light inhibition for M2→LS and M1→LS, light and dark blue, respectively. **C**, upper panels, Effect of the inhibition of the premotor or primary motor cortico-striatal projection on the transition time for self-paced sequences. **D**,  $\Delta$  on-off for the inhibition before and execution protocols from the inhibition of M2→LS presented in Figures 4, 5, respectively. **E**, No effect was detected by the inhibition of either M2→LS or M1→LS projection in the different categories of errors. Upper panels 1–4, Quantification per animal in off versus on trials of the proportion of each category of error. In **C**, **E**, each line in the paired plots depicts the mean effect per animal during trials of optogenetic inhibition (on; green shadow) versus trials without optogenetic inhibition (off; no shadow) from the same session. The panels  $\Delta$  on-off are obtained from the mean difference per animal in the on-off trials, adding the control group in gray. The mean difference  $\Delta$  in change score panels (mean d.) are obtained between the experimental groups and the control group (see Materials and Methods). Paired plots, two-sided permutation *t* test; panels  $\Delta$  on-off, Arch animals versus control eYFP animals, unpaired two-sided permutation *t* test; \**p* < 0.05. The exact *p* values are described in the text and Table 1.



**Movie 1.** Execution of a forced sequence. [View online]



**Movie 2.** Execution of a self-paced sequence. [View online]



**Movie 3.** Example of a broken sequence after light inhibition before the initiation of the sequence. [View online]

$p = 0.65$ , Friedman test, wild-type (WT) animals,  $n = 8$ , Fig. 1E]. No differences were found in comparisons of a number of task-relevant parameters between forced versus self-paced sequences: latency to initiate, the transitions intrasubsequences, the intervals between presses intra subsequences ( $p > 0.05$ , Mann–Whitney  $U$  test, WT animals,  $n = 8$ ; Extended Data Fig. 1-1A).

While animals executing forced sequences reached an  $83 \pm 1.5\%$  in correct performance (correct sequences/errors + correct sequences), the execution of self-paced sequences only reached  $61 \pm 1.7\%$  (WT animals,  $n = 8$ ; Fig. 1E, red and blue tick curves, respectively). To further investigate this performance, we quantified the types of errors and modes in which the animals executed correct sequences. An error was defined as a sequence of presses in which the animal did not achieve four presses on lever 1 followed by four presses on lever 2. The errors were grouped into four categories: (1) incorrect start (starting on the opposite lever); (2) breaks in S1; (3) premature switches from S1 to S2; and (4) breaks in S2 (Fig. 1B,C, right panels 1–4, respectively; note that 1 and three were only possible during self-paced). These four categories were quantified late in training (Fig. 1G). The decrease in Breaks in S1 and S2 was the primary determinant in performance improvement of both forced (ForcBreaks) and self-paced (S-PBreaks) sequences compared with pretraining ( $p < 0.05$ , Mann–Whitney  $U$  test, WT animals,  $n = 8$ ; Extended Data Fig. 1-1B, panels 2, 4). A decrease in incorrect-start errors accounted for the major improvement in the self-paced performance ( $p = 0.007$ , Mann–Whitney  $U$  test, WT animals,  $n = 8$ ; Extended Data Fig. 1-1B, panel 1). No difference in performance between forced and self-paced sequences was detected when accounting for only the available errors in both forced and self-paced sequences: BreaksS1+BreaksS2 ( $p = 0.5$ , Mann–Whitney  $U$  test, WT animals,  $n = 8$ ; Fig. 1E, blue dashed curve vs red curve).

The correct execution in forced sequences was  $S1 = 4 \rightarrow S2 = 4$ ; in self-paced the execution of correct sequences grouped in several options (as anything with  $S1 = >4 \rightarrow S2 \geq 4$  was correct). The majority of correct



**Movie 4.** Example of return to start after light inhibition before the initiation of the sequence. [View online]

sequences were Long-S1 sequences ( $S1 > 4 \rightarrow S2 \geq 4$ ; WT animals,  $n = 8$ ; Fig. 1F).

Besides the execution structure of the sequences, we quantified the length parameters. The latency to start, the transition between subsequences, the interpress intervals, the duration, all became faster as training progressed (Friedman test,  $p < 0.05$ ; WT animals,  $n = 8$ ; Extended Data Fig. 1-1A). Later in training, the latency to initiate the sequences was not different between forced and self-paced (forced:  $1.1 \pm 0.1$  s, self-paced:  $1.5 \pm 0.3$  s,  $p = 0.535$ , Mann–Whitney  $U$  test, WT animals,  $n = 8$ ; Fig. 1H). Neither the transition time between subsequences ( $S1_{end} \rightarrow S2_{start}$ ) or the interpress intervals intersubsequences ( $p > 0.05$ , Mann–Whitney  $U$  test; Fig. 1J,K). However, the duration and the number of presses were longer in the S1 of self-paced than in forced [forced<sub>duration</sub>:  $3.2 \pm 0.2$  s vs self-paced<sub>duration</sub>:  $4.8 \pm 0.4$  s, forced<sub>S1presses</sub> =  $4 \pm 0$  vs  $6.1 \pm 0.6$  in self-paced<sub>S1presses</sub>,  $p = 0.0002$ , Mann–Whitney  $U$  test; Extended Data Fig. 1-1C,D).

This task parameterization showed that mice could learn and execute forced and self-paced serial order sequences in blocks. The main difference in the execution of these two modes of sequences (besides that self-paced have more possibilities for errors) is that animals execute longer chunks of presses in the subsequence 1 of self-paced sequences.

### Activity modulation in premotor and motor cortical neurons during the execution of serial order sequences

Once we established that mice are capable of executing serial order sequences, we questioned if, as predicted, the activity of M2 and M1 cortical neurons was modulated during the execution of these trained sequences (Tanji and Evarts, 1976; Mushiaki et al., 1990; Churchland et al., 2006; Shima et al., 2007). For this purpose, we trained eight animals as in Figure 1. After 3 d in the blocks of forced–self-paced sessions, we performed brain surgeries to implant a mobile electrode array either in M2 ( $n = 6$ ; Fig. 2A, middle panel) or M1 ( $n = 2$ ; here, we verified the region to evoke forepaw movements by micro-

stimulation; see Materials and Methods; Fig. 2A, right panel). After 4 d of recovery, the training restarted until animals reached a stable performance in the execution of forced and self-paced sequences (10–15 blocks sessions postsurgery). From these animals, 34 well-isolated units in M2 and 26 units in M1 were analyzed. Representative examples of these neurons' activity during the executions of sequences are presented in Figure 2B,C. The z score heatmaps of Figure 2D,E show all recorded units during the execution of self-paced sequences (the same units during the execution of forced sequences are presented in Extended Data Fig. 2-1).

To answer whether the same units were active during the different phases of the sequences, we measured the mean activity of neurons above two z scores during the execution of the sequences. We classified neuronal activity into categories based on different parameters of sequence execution (Fig. 2F). We found no statistical difference in the comparison of M2 versus M1 activity, only a tendency for more modulated/engaged M2 neurons related to the initiation of a sequence (Fig. 2G). To explore this difference during sequence initiation, we compared the mean z score between M2 and M1 activity from the units that showed a significant modulation 1 s before starting the sequences (Fig. 2H,I). This comparison showed a bigger z score positive modulation in M2 than in M1 during the execution of the sequences (M2 = 14 of 34 units, M1 = 8 of 26 units; mean z score in self-paced sequences:  $M2_{S1} = 1.32$ ,  $M2_{S2} = 0.85$  vs  $M1_{S1} = 0.55$ ,  $M1_{S2} = 0.22$ ;  $p < 0.05$ , z score difference test; Fig. 2J, bars labeled "S1 and S2"). Remarkably M2 units showed a stronger modulation in self-paced sequences, even before the initiation of the sequence ( $M2_{S-Init} = 1.4$  vs  $M1_{S-Init} = 0.8$ ,  $p = 0.04$  z score difference test; Fig. 2J, bars labeled "Init" in blue) and a similar tendency during the initiation of forced sequences (Extended Data Fig. 2-1H, bars labeled "Init" in red). No difference in the number of recruited units throughout the execution of the sequences was detected ( $p > 0.05$ ,  $\chi^2$  test; Extended Data Fig. 2-1).

### Both M2 and M1 contain units encoding the length of the serial order sequences of actions

After the evaluation of the mean z score related to the execution of the serial order sequences, we tested the hypothesis that M2/M1 encode the length parameters of the execution of these sequences (Riehle and Requin, 1989; Riehle et al., 1994; Lucchetti and Bon, 2001; Sakurai et al., 2004; Churchland et al., 2006; Jin et al., 2009; Hernández et al., 2010; Merchant et al., 2013; Crowe et al., 2014; Murakami et al., 2014; Mendoza et al., 2018). To evaluate this possibility, we performed linear regressions between the duration of the segments of the sequences (total sequence, S1, transition, or S2) and the neural activity recorded from individual neurons in either M2 or M1. We reasoned that if these cortices contained activity encoding the sequence length, their cortico-striatal projections could convey this information to the striatum.

Figure 3A shows two examples of units that presented significant regressions ( $R^2 > 0.6$  and  $p < 0.05$ ) in specific time bins during the execution of serial order self-paced

sequences (Fig. 3A, middle row panels, gray shadows). Figure 3B shows the proportion of units that presented with significant regressions based on five questions: column i, does the activity before the first press (1 s) encode the sequences' length? ii, does the mean activity during the sequence encode the length of the sequence? iii, iv, and v, Is there a relationship between the duration of S1, the transition or the duration of S2, and the mean firing rate during these epochs? The answer to these five questions is presented per recorded unit in either M2 or M1 (Fig. 3B, upper panels) and as the % of units with significant regressions per region (Fig. 3B, bottom panels). Notably, the biggest proportion of units with significant regressions was between the sequence duration and the firing rate before the initiation of the sequence in both M2 and M1 (Fig. 3B, columns i) or the sequences duration and the mean firing rate of M2 during the sequences (Fig. 3B, columns ii).

The percentage of recruited units over time (units presenting significant regressions, 200-ms bin, sliding 10 ms;  $R^2 > 0.6$  and  $p < 0.05$ ) is presented in Extended Data Figure 3-1B. Despite small tendencies, no difference was detected in the proportion of units recruited overtime either when comparing M2 versus M1 nor when comparing within each region between forced and self-paced sequences (1 s before or one after the start of the sequences). Similarly, no differences were found between neuronal activity and the duration of the sequence, duration of S1, duration of the transition, or the number of presses (comparison of bars  $p > 0.05$ ,  $\chi^2$  test; Extended Data Fig. 3-1B).

To address whether specific cortico-striatal M2 or M1 neurons encode for sequence parameters, we recorded from antidromic photo-identified cortico-striatal neurons *in vivo* (Lima et al., 2009; Díaz-Hernández et al., 2018). To achieve this, we first confirmed the lateral region of the striatum (LS) that is innervated by both M2 and M1 projections (Extended Data Fig. 3-2A–D; Oh et al., 2014; Sohur et al., 2014; Hintiryan et al., 2016; Hunnicutt et al., 2016). Then we trained mice in which the expression of Channelrhodopsin-2 (ChR2) was targeted to the excitatory cortical neurons in M2 ( $n = 4$ ) or M1 ( $n = 2$ ) and their projections to the striatum (using Emx1-Cre mice; Guo et al., 2000; Gorski et al., 2002). We then implanted an electrode array above the ChR2 expression and an optical fiber into LS to antidromically activate the cortico-striatal units (Extended Data Fig. 3-2E–G; Friedman et al., 2015). Following this procedure and after a stable performance in the execution of blocks of forced–self-paced sequences, the activity of M2 or M1 units was recorded. During these recordings, we recorded cortical and cortico-striatal photo-identified units (PID units). A PID unit was that, at the end of the session, responded to antidromic light stimulation with short latency ( $< 10$  ms; Díaz-Hernández et al., 2018). The mean latency of M2+M1→LS was  $5.1 \pm 0.4$  ms;  $n = 21$ ; Extended Data Fig. 3-2F, bottom right panel). Following these criteria, we identified 10 M2 and 11 M1 cortico-striatal PID units (Extended Data Fig. 3-2G). As in the non-PID units (Fig. 3B), the major proportion of PID units presented significant regressions between the sequences duration and the firing rate before

the initiation, the duration, and the mean firing rate during the execution of the sequences (Extended Data Fig. 3-2G, columns i, ii).

In summary, in Figures 2, 3 and Extended Data Figure 3-2, we show that the activity of M2 and M1 is related to the execution of the trained sequences. The mean z score analysis showed that M2 had a bigger modulation than M1 during the execution and even before the initiation of the serial order sequences. Furthermore, the regression analysis showed that both M2 and M1 contain units that encode the sequences' execution length.

### Inhibition of lateral striatal neurons before initiation of a serial order sequences impairs its execution

This study's main goal was to establish whether cortico-striatal projections of the premotor and motor cortex contribute to the execution of sequences. To address this point, we first verified that neuronal activity in the lateral striatal (LS) region that receives inputs from M2 and M1 (Extended Data Fig. 3-2A-D) contributes to the execution of serial order sequences. For this purpose, we trained a group of animals in which the inhibitory opsin archaerhodopsin (Arch3.0) was injected bilaterally into LS followed by fiber-optic implantation above the injection sites (Extended Data Fig. 4-1A). Then, once the animals reached around 80% success (correct sequences) in the performance of forced and 60% in self-paced sequences (Extended Data Fig. 4-1A, panel 3), we performed sessions of optogenetic inhibition, delivering the light to inhibit Arch3.0-expressing neurons in a state-dependent manner during the execution of the sequences. We randomized three protocols (each protocol on a different day): (1) before the initiation; (2) during the execution; or (3) during the transition between subsequences (Extended Data Fig. 4-1B-G, H-M, N-S, respectively). We observed that optogenetic inhibition before starting the sequence delayed the initiation (Extended Data Fig. 4-1C). Inhibition during the execution of the sequence increased premature switches (Extended Data Fig. 4-1J, panel 3) and decreased the correct Long-S1 self-paced sequences (Extended Data Fig. 4-1K). Inhibition during the intersubsequence transitions increased the transition time between forced subsequences and showed a tendency to increase the time between self-paced subsequences (Extended Data Fig. 4-1R). Note that the data for the forced sequences are only presented in the figures when significant effects were detected; otherwise, they are presented only in Table 1.

### Presequence initiation inhibition of either motor or premotor cortico-striatal projections impairs initiation, but only the latter disrupts the execution

Once we verified that direct inhibition of LS neurons impaired the execution of sequences, we asked whether the premotor (M2→LS) or the motor (M1→LS) cortico-striatal projections contributed to the execution of these sequences. We first verified the inhibition of striatal neurons by the optogenetic inhibition of cortico-striatal projections using Arch3.0 with 2-s pulses of light (Fig. 4A). This pulse length is in a proper range far from the biophysical constraints of using Arch for optogenetic inhibition (Mahn et al., 2016;

Díaz-Hernández et al., 2018). Furthermore, we evaluated the proportion of labeled cells in M2/M1 that contain corticofugal axons crossing by the area of the LS manipulations (Extended Data Fig. 4-2).

Next, we tested whether the contribution of cortico-striatal projections is time dependent (Bartolo et al., 2014; Bartolo and Merchant, 2015; Li et al., 2016; Nakayama et al., 2018). We performed optogenetic inhibitions of the M2→LS ( $n = 9$ ) or M1→LS ( $n = 8$ ) projections in a state-dependent manner, using three protocols: (1) before initiation (Fig. 4); (2) during execution (Fig. 5); and (3) during the transition between subsequences (Fig. 6).

Most of the effects of optogenetic inhibition were on self-paced sequences. Therefore, for Figures 4-6, forced sequences are only presented when effects were detected; otherwise, only self-paced sequences are presented. The full data for forced and self-paced inhibitions is in the Table 1.

To carry out these experiments, a group of Emx1-Cre mice was subject to bilateral Arch3.0-eYFP expression into M2 or M1 (or eYFP for control animals) and bilateral fiber optic implantation into the LS (Fig. 4B; see Figs. 4-6). After surgery, animals were allowed to recover for 3 d before training started and continued until the performance was stable (Fig. 4D). During the optogenetic inhibition sessions, and depending on the protocol, a continuous pulse of green light was applied randomly in 50% of the trials (2 s; triggered by the behavior), allowing us to compare the effects of light inhibition on each animal within the same session.

For the inhibition "before" initiation protocol, we aimed to assess whether the cortico-striatal projections contribute to sequence execution by interfering with the initiation/preparation of the sequences for which we took advantage of the stereotyped behavior of the trained animals. An infrared beam was placed between the magazine and the levers (red arrow-dashed line coming out of the magazine; Fig. 4C), it was possible to trigger a pulse of light when the animal crossed the infrared beam before starting the sequences (Tecuapetla et al., 2016).

The inhibition of the M2→LS projections before initiation increased premature switches ( $M2 \rightarrow LS_{\text{Self-pacedOn}} = 20 \pm 5$  vs  $M2 \rightarrow LS_{\text{Self-pacedOff}} = 8 \pm 1$ ; the paired mean difference was 12.2 [95.0%CI 6.8, 27] and  $p = 0.0001$ ,  $q = 0.01$  two-sided permutation  $t$  test; Fig. 4E, panel 3, light blue data; Movie 3). This effect was not observed in control animals ( $\Delta$  on-off comparison to the control group: the unpaired mean difference between control and M2→LS was 10.4 [95.0%CI 3.7, 2.4]. The  $p$  value of the two-sided permutation  $t$  test was 0.0224,  $q = 0.06$ ; Fig. 4F, panel 3, bottom part). The increased premature switches were accompanied by decreased presses within the self-paced sequence ( $M2 \rightarrow LS_{\text{Self-pacedOn}} = 9 \pm 0.6$  vs  $M2 \rightarrow LS_{\text{Self-pacedOff}} = 10 \pm 0.4$ ; the paired mean difference was  $-1.16$  [95.0%CI  $-2.42, -0.495$ ],  $p = 0.016$ ,  $q = 0.05$  two-sided permutation  $t$  test; Fig. 4F, light blue data).

This inhibition protocol also increased the latency to start the sequences ( $M2 \rightarrow LS_{\text{Self-pacedLatencyOn}} = 2.9 \pm 0.4$  vs  $M2 \rightarrow LS_{\text{Self-pacedLatencyOff}} = 1.8 \pm 0.3$ ; the paired mean difference was 1.1 [95.0%CI 0.556, 1.96],  $p = 0.0026$ ,  $q = 0.01$  two-sided permutation  $t$  test; Fig. 4G, light blue

left panel; forced sequences were also delayed, see Table 1, data related to Fig. 4), an effect not observed in control animals (Fig. 4G,  $\Delta$  on-off panel, gray data). This increased latency to start was accompanied by an increase in the animals' return to the magazine in the trials that received light inhibition, suggesting that inhibition interrupted the proper serial order sequence initiation (see Movie 4;  $M2 \rightarrow LS_{SP\text{-}returns\_to\_startON} = 9 \pm 2\%$  vs  $M2 \rightarrow LS_{SP\text{-}returns\_to\_startOff} = 1 \pm 0.7\%$ , the paired mean difference between control and  $M2 \rightarrow LS$  was  $8.29$  [95.0%CI 5.14, 11.7],  $p = 0.006$ ,  $q = 0.03$  two-sided permutation  $t$  test. Unpaired mean difference between control and  $M2 \rightarrow LS$  was  $9.86$  [95.0%CI 6.0, 13.8],  $p = 0.0002$ ,  $q = 0.002$  two-sided permutation  $t$  test; Fig. 4G,  $\Delta$  on-off panel).

Conversely to the inhibition of  $M2 \rightarrow LS$  projections, the increase in premature switches and the decrease in the number of presses within the sequence were not observed when we inhibited  $M1 \rightarrow LS$  projections (Fig. 4E,F, dark blue data). Instead the inhibition of the  $M1 \rightarrow LS$  projections increased the latency to start the self-paced sequences ( $M1 \rightarrow LS_{Self\text{-}paced\_LatencyON} = 3.2 \pm 0.4$  vs  $M1 \rightarrow LS_{Self\text{-}paced\_LatencyOff} = 2.6 \pm 0.3$ ; the paired mean difference was  $0.614$  [95.0%CI 0.40, 1.1] and  $p = 0.009$ ,  $q = 0.04$  of the two-sided permutation  $t$  test; Fig. 4G, comparison to control: panel  $\Delta$  on-off same figure, dark blue vs gray data, unpaired mean difference between control and  $M1 \rightarrow LS$  was  $0.88$  [95.0%CI 0.4, 1.7] and  $p = 0.003$ ,  $q = 0.01$  of the two-sided permutation  $t$  test), and the returns to start (comparison to control: panel  $\Delta$  on-off in the same figure, dark blue vs gray data; unpaired mean difference between control and  $M1 \rightarrow LS$  was  $11.8$  [95.0%CI 3.3, 26.1] and  $p = 0.02$ ,  $q = 0.06$  of the two-sided permutation  $t$  test; Fig. 4H).

Together these results suggest that the  $M2 \rightarrow LS$  but not the  $M1 \rightarrow LS$  projections contribute to the execution/structuring of self-paced sequences while both  $M2 \rightarrow LS$  and  $M1 \rightarrow LS$  contribute to the initiation.

### Inhibition of premotor cortico-striatal projections at the start of the execution decreased Long-S1 sequences

One prediction for the cortico-striatal projections' contribution to serial order sequences execution is that their requirement would be time dependent (see Figs. 2, 3; Li et al., 2016; Nakayama et al., 2018). To further prove this idea, we performed a second protocol: inhibition during "execution," which consisted of performing light inhibition of the cortico-striatal projections once the execution of the sequences started (triggered by the first press in S1; Fig. 5A). Using this protocol, we observed that the inhibition of the  $M2 \rightarrow LS$  projections did not modify the proportion of the different categories of errors (Fig. 5B) nor the number of presses in the sequences (Fig. 5C), but it did decrease the proportion of Long-S1 sequences ( $M2 \rightarrow LS_{Long\_S1\_SeqON} = 35 \pm 5$  vs  $M2 \rightarrow LS_{Long\_S1\_SeqOff} = 50 \pm 6$ , the paired mean difference was  $-14.6$  [95.0%CI  $-18.9$ ,  $-9.8$ ] and  $p = 0.002$ ,  $q = 0.04$  of the two-sided permutation  $t$  test; Fig. 5D, upper panels; comparison to control eYFP-group:  $\Delta$  on-off panel, unpaired mean difference

between control and  $M2 \rightarrow LS$  was  $-18.4$  [95.0%CI  $-28.3$ ,  $-8.8$ ]  $p = 0.003$ ,  $q = 0.04$  of the two-sided permutation  $t$  test (Fig. 5D, bottom panel), with no overall effect on the duration or the number of presses in the sequences (see Table 1; data related to Fig. 5). The inhibition of the  $M1 \rightarrow LS$  projections did not yield any significant effects with the inhibition during execution protocol (Fig. 5, dark blue data).

The results from the inhibition of  $M2 \rightarrow LS$  or  $M1 \rightarrow LS$  projections during the beginning of the sequence execution highlight that the activity of the  $M2 \rightarrow LS$  projections is important for the length of the sequences (particularly for S1). Furthermore, these results also suggest that, at least later in training, the  $M1 \rightarrow LS$  projections are not required for sequence execution.

### Inhibition of premotor cortico-striatal projections during the transition between serial order subsequences increases the transition time

So far, we have shown that the cortico-striatal projections from  $M2 \rightarrow LS$  contribute to the appropriate initiation and execution of self-paced serial order sequences (Figs. 4, 5). However, in the previous experiments, the light inhibition never occurred during the transition between subsequences. Given that a small proportion of units from either  $M2$  or  $M1$  showed significant modulation during the transition-moment (Fig. 2F,G), we asked whether inhibiting directly during the transition could reveal whether the  $M2 \rightarrow LS$  or  $M1 \rightarrow LS$  contribute to the transition. For this purpose, we set up an inhibition during "transition" protocol, in which the press before the penultimate press of S1 triggered light inhibition for 2 s (Fig. 6A, for self-paced; in forced sequences, it was the third press; see Table 1, data related to Fig. 6).

Figure 6B shows the mean press in which the animals of the  $M2 \rightarrow LS$  or the  $M1 \rightarrow LS$  groups received the inhibitory stimulation (or the corresponding timestamp in the "off" trials); on average, it was the press  $-2$  counting from the final press in the S1 ( $M2 \rightarrow LS_{transition\_lightON} = -2.0 \pm 0.1$  vs  $M2 \rightarrow LS_{transition\_lightOff} = -1.9 \pm 0.1$ ,  $p = 0.25$ , Mann-Whitney  $U$  test; Fig. 6B). With this protocol, we observed that the inhibition of  $M2 \rightarrow LS$ , but not  $M1 \rightarrow LS$ , showed a tendency to increase the duration of the transition ( $M2 \rightarrow LS_{TransitionON} = 1.0 \pm 0.06$  vs  $M2 \rightarrow LS_{TransitionOff} = 0.8 \pm 0.06$ , the paired mean difference was  $0.08$  [95.0%CI 0.02, 0.16] and  $p = 0.050$ ,  $q = 0.4$  of the two-sided permutation  $t$  test; Fig. 6C, upper panels), that reached significance when compared with the eYFP-control group: unpaired mean difference between control and  $M2 \rightarrow LS$  was  $0.18$  [95.0%CI  $-0.09$ ,  $0.3$ ] and  $p = 0.003$ ,  $q = 0.03$  of the two-sided permutation  $t$  test; Fig. 6C,  $\Delta$  on-off bottom panel). This effect was time-specific since neither the inhibition before nor the inhibition execution protocol on the  $M2 \rightarrow LS$  yielded a similar effect (Fig. 6D). This effect on the transition raised the question of whether the  $M2 \rightarrow LS$  projections treat each subsequence as independent chunks or concatenate them into a single chunk once the whole sequence has been acquired (Geddes et al., 2018; Martiros et al., 2018). We hypothesized that if the transition was affected by the light inhibition, the proportion of breaks in the sequences might increase as well. Contrary to this hypothesis, no modifications on the breakings of sequences

were detected by this protocol (Fig. 6E). We also observed no differences in the number of presses or sequence length (Table 1), supporting the idea that the M2→LS projections contribute to the transition intersubsequences without affecting the second part of the serial order sequence.

Altogether, the results from the recording and inhibition experiments reveal that the cortico-striatal projections to the LS from the premotor and motor cortices have specific contributions to the execution of sequences. Both projections contribute to the initiation, while M2→LS also contributes to the correct execution and transition between subsequences of self-paced sequences. Importantly the M2→LS contribution was essential during the beginning of the execution, suggesting its contribution is relevant before the initiation, at the beginning of execution, and decreasing in relevance as the sequence execution progressed.

### Premotor cortico-striatal projections innervate the direct pathway with a stronger synaptic weight than the indirect pathway

Finally, we investigated whether the M2→LS projections differentially impact the two subcircuits of striatal projection neurons, the direct or indirect striatal pathways (Wall et al., 2013), by looking at synaptic connectivity. For these experiments, we crossbred Emx1-Cre (allowing us to express Chr2 in M2) with BAC D2-GFP mice. By injecting red retrobeads into the substantia nigra, we could identify in the striatum neurons from direct pathway (red retrobeads; dMSN), or the indirect pathway (GFP; iMSN). This allowed us to record from identified striatal neurons in brain slices *ex vivo* while stimulating the M2→LS Chr2 axons (Extended Data Fig. 4-3). Using this procedure, we recorded pairs of neurons in the same brain slice in the LS (one iMSN and one dMSN; counterbalancing the recording order per slice). We evoked postsynaptic responses by activating the M2→LS Chr2 projections with brief pulses of light (1 ms; Extended Data Fig. 4-3C). From these experiments, we recorded a total of 6 pairs of striatal neurons (in 6 different slices from four animals). Postsynaptic evoked responses had a bigger amplitude in the dMSN than in the iMSN (dMSN:  $290 \pm 100$  vs iMSN =  $30 \pm 9$  pA, Mann-Whitney *U* test,  $p = 0.031$ ; Extended Data Fig. 4-3F), with no difference in their latencies (dMSN:  $3.3 \pm 0.1$  ms vs iMSN =  $3.8 \pm 0.1$  ms, Mann-Whitney *U* test,  $p > 0.05$ ; Extended Data Fig. 4-3F). These evoked postsynaptic responses were glutamatergic, being blocked by the AMPA receptor antagonist CNQX (Extended Data Fig. 4-3G). This finding suggests that the M2→LS projections may have stronger synaptic connections onto the dMSNs than onto the iMSNs *in vivo* when the animals are executing the serial order action sequences.

## Discussion

These results show that mice can execute serial order forced and self-paced sequences of lever presses (Fig. 1). Both the premotor (M2) and motor (M1) cortices are modulated during sequence execution (Fig. 2). M2 showed a bigger modulation during the initiation and execution in the units modulated before the start of the sequences (Fig. 2J). Both M2 and M1 units showed regressions between their

activity and the sequence duration before or during the execution (Fig. 3B), even in photo-identified M2 and M1 cortico-striatal cells (Extended Data Fig. 3-2G). The M2→LS and M1→LS projections contribute to the proper initiation, but mainly M2→LS projections contribute to the structuring/execution of serial order self-paced sequences (Figs. 4-6). The M2→LS synapses present bigger amplitude postsynaptic responses onto the direct versus the indirect pathway of striatal neurons (Extended Data Fig. 4-3).

Mice had been previously been shown to develop and execute serial order operant tasks, including pressing two levers (Geddes et al., 2018; Rothwell et al., 2015). The task adapted here allows temporally separated manipulations within the different phases of the two subsequences (initiation, execution, and transition between subsequences). We first trained animals in forced sequences and later in blocks of forced-self-paced sequences as animals trained only in the latter dropped their behavior. The fact that animals were more efficient at executing forced than self-paced can be explained by the greater number of possible errors in self-paced sequences. However, a difference in the recruitment of brain structures in forced versus self-paced sequences is not excluded (Romo and Schultz, 1992; Hernández et al., 2010).

To identify whether the cortico-striatal projections from M2/M1 contribute to sequence execution, we investigated whether neuronal activity in these structures was modulated during the execution of the sequences. We identified that M2 and M1 units showed activity modulations milliseconds before the start and during the execution of these serial order sequences (Figs. 2, 3), with mostly exclusive firing categories (Fig. 2F). Importantly, the units from M2 that were modulated before the sequences started showed a bigger positive modulation during the execution and before starting the sequences than those from M1 (Fig. 2J). This increased activity time before the execution of movements is attributed to time estimation or preparation to execute an action [e.g., the anticipatory activity (ramping) in M2 has a direct relationship with the time that animals wait to start an action or the duration of a stimulus (Murakami et al., 2014; Mendoza et al., 2018)]. In this study, the animals had to approach the lever before the first press in the sequence. We could not therefore rule out that the activity before starting the sequences may be related to motor preparation, although the inhibition of this activity before pressing delayed the latency of both forced and self-paced sequences, but only impaired the execution of self-paced sequences. Together, these results show that units in M2/M1 are modulated during the execution of sequences. When evaluating whether these units' activity may encode the execution parameters, we observed no significant differences in the proportions of units in M2 versus M1, as measured by regression analysis between neuronal activity and temporal parameters of the sequences (Fig. 3B). These results show that both M2 and M1 contain units encoding the sequences' execution (Nelson et al., 2020; Berlot et al., 2021). However, it must be acknowledged that the lack of differences in some of the comparisons between M2 and M1 may be

influenced by the small set of recorded cells (34 cells from M2 and 26 from M1).

To evaluate how the M2/M1 cortico-striatal projections contribute to the execution of serial order sequences, we performed two experiments. First, we recorded from cortico-striatal antidromic PID units (Extended Data Fig. 3-2). Second, we performed state-dependent temporal inhibitions of the M2→LS or the M1→LS projections either before or during the execution of sequences (Figs. 4-6). Although the photo-identification of cortico-striatal M2→LS or M1→LS was low (10 per structure), it allowed us to detect units in each of these cortices that presented significant regressions with temporal parameters of the execution of the sequences. However, there were too few photo-identified neurons to infer whether M2 or M1 has a more important contribution to sequences execution. The contribution of these cortico-striatal projections was thus mainly evaluated with state-dependent optogenetic inhibition.

To test the hypothesis that the M2/M1 cortico-striatal projections have time-specific contributions to sequences execution, we performed three protocols of inhibition while animals performed lever pressing sequences. Our inhibitions were all 2 s, below the safe limit of the biophysical constraints of using Arch for optogenetic inhibitions (Mahn et al., 2016).

Interestingly, the inhibition of either the M2→LS or M1→LS, before the initiation increased the latency to start the sequences (Fig. 4G). This increase in latency was accompanied by an increase in the animals' return to the magazine in the initiations that received light inhibition, as if the inhibition interrupted the proper initiation (Fig. 4H; see Movie 4). These results are consistent with a model where the M2→LS and M1→LS cortico-striatal projections are required for the proper initiation of sequences, with the former likely setting up the parameters for the upcoming sequence (for further discussion, see below).

Remarkably, the three inhibition protocols revealed that the projections from M2→LS, but not the M1→LS, are temporally required for the execution of self-paced sequences. The inhibition of M2→LS before the start altered the sequence structure, increasing premature switches (Fig. 4E) and decreasing the number of actions in the sequence (Fig. 4F). Their inhibition during the beginning of the execution affected the first segment of the sequence (by decreasing the probability of executing Long-S1 sequences; Fig. 5D). Their inhibition during the transition increased the transition time between subsequences, although this last had the slightest effect (Fig. 6C).

A previous experiment, which decreased the M2→striatal projections (by manipulating M2→striatal projections plus their collaterals to other brain regions) during the execution of a serial order short sequence reported that inhibition of M2→dorsolateral striatal cells, retrogradely labeled from the striatum, impaired the first step accuracy (Rothwell et al., 2015), perhaps by increasing incorrect starts or promoting premature switches from S1 to S2. Here, the possibility of longer subsequences in the sequence allowed for measuring incorrect starts, breaks, premature switches, and the transition time between subsequences. Our inhibitions of M2→LS was spatially and temporally specific (if the optogenetic

inhibition does not backpropagate as it has been documented; El-Gaby et al., 2016), showed no effect on incorrect starts. Rather we observed an increase in premature switches when inhibiting before the start, a decrease in Long-S1 sequences when inhibiting during the execution, and slowness of the transition time when inhibiting around the transition.

Another important point reported here is the specificity of the effects mainly on self-paced sequences (see Table 1). How is it that the premotor projections can differentiate between the execution of forced and self-paced sequences? A possible explanation is that the M2→LS projections could detect whether the animals were in blocks of self-paced sequences, engaging these projections with a bigger sensitivity to the inhibitions as a consequence of self-deciding the execution. This possibility is supported by previous studies showing that when animals engage in self-paced behaviors, as opposed to forced behaviors, some cortical subcircuits become engaged and more important (Romo and Schultz, 1992; Hernández et al., 2010; although see Kurata and Tanji, 1985; Thaler et al., 1988). An idea supported by the tendency of cortico-striatal M2 PID units to show a bigger proportion of units with significant regression in the self-paced sequences (Extended Data Fig. 3-2G, columns i, iii). Importantly we observed that the inhibition of the M1→LS did not affect the execution of sequences, consistent with the idea that M1→LS activity is not required to execute sequences once these have been learned (Kawai et al., 2015).

Finally, another remarkable finding from the optogenetic inhibitions experiments is that the M2→LS projections may contribute as a serial driver of sequence execution (Lashley, 1951; Zeigler and Gallistel, 1981; Graybiel, 1998; Rosenbaum et al., 2007; Jin and Costa, 2015). Supporting this idea, their inhibition before the starting could restart the initiation, increasing premature switches during the execution, and decreasing the number of actions (Fig. 4E,F). Conversely, their inhibition during the start of the execution decreased the probability of executing Long-S1 sequences only (Fig. 5D).

In addition to the inhibition of cortico-striatal projections, we verified the LS requirement for the sequence execution and addressed the possibility that our cortico-striatal inhibitions may affect other brain areas besides the LS by performing two experiments: (1) we directly inhibited the lateral striatal neurons with the same protocols that inhibited the cortico-striatal projections (Extended Data Fig. 4-1); and (2) we evaluated whether the manipulated region contains axons en passant from M2/M1 that reach other brain areas (e.g., thalamus/pons; Th/Pns; Extended Data Fig. 4-2).

The first experiment's results found that direct inhibition of LS during sequence execution decreased the length of correct sequences (Long-S1 sequence) and the number of presses (Extended Data Fig. 4-1K,M). The inhibition of the LS in the transition protocol increased the transition time between subsequences (Extended Data Fig. 4-1R). These effects were in line with the inhibition of M2→LS projections. However, the LS inhibition before the sequence start did not change the errors in self-paced sequences, contrary to the inhibition of the M2→LS projections which increased premature switches with this protocol. A possible explanation for

**Table 1: Descriptive statistics and data extended from the main figures**

	Panel/data	Descriptive statistics	Type of test	<i>p</i> value	<i>n</i>
Data related to Figure 4	Breaks S1	Mean ± SEM (%)			
		Forced off vs forced on			
		M2-LS: 0 ± 0 vs 1.8 ± 0.9; M1-LS: 0.8 ± 0.8 vs 2.3 ± 1.2; controls: 0 ± 0 vs 2.6 ± 1.4	Paired two-sided permutation <i>t</i> test	1; 1; 1	Emx1-cre mice (+/-)
		Forced: change rate (on-off)			
	Breaks S2	M2-LS: 1.8 ± 0.9 vs controls: 2.6 ± 1.4	Unpaired two-sided permutation <i>t</i> test	0.68	AAV-Arch-M2-LS: <i>n</i> = 9
		M1-LS: 1.4 ± 0.8 vs controls: 2.6 ± 1.4	Unpaired two-sided permutation <i>t</i> test	0.49	AAV-Arch-M1-LS: <i>n</i> = 8
		Mean ± SEM (%)			Control:
		Forced off vs forced on			AAV-eYFP-M2-LS: <i>n</i> = 9
	Sequence	M2-LS: 13.7 ± 3.3 vs 7.8 ± 2.9; M1-LS: 12 ± 6 vs 19 ± 7; controls: 17 ± 4 vs 14 ± 3	Paired two-sided permutation <i>t</i> test	0.1; 0.3; 0.2	
		Forced: change rate (on-off)			
		M2-LS: 5.8 ± 3 vs controls: -3 ± 2.6	Unpaired two-sided permutation <i>t</i> test	0.84	
		M1-LS: 6.9 ± 6 vs controls: -3 ± 6.9	Unpaired two-sided permutation <i>t</i> test	0.79	
	Latency	Mean ± SEM (# presses)			
		Forced off vs forced on			
		M2-LS: 8.3 ± 0.1 vs 8.4 ± 0.2; M1-LS: 8.1 ± 0.2 vs 8 ± 0.1; controls: 8.1 ± 0.1 vs 8 ± 0.1	Paired two-sided permutation <i>t</i> test	0.8; 0.6; 0.7	
		Forced: change rate (on-off)			
	Return to start	M2-LS: 0.07 ± 0.3 vs controls: -0.03 ± 0.09	Unpaired two-sided permutation <i>t</i> test	0.84	
		M1-LS: -0.08 ± 0.1 vs controls: -0.03 ± 0.09	Unpaired two-sided permutation <i>t</i> test	0.79	
		Mean ± SEM (s)			
		Forced off vs forced on			
Performance	M2-LS: 1.4 ± 0.1 vs 2.4 ± 0.3; M1-LS: 2.9 ± 0.6 vs 3.6 ± 0.6; controls: 2.0 ± 0.4 vs 1.8 ± 0.3	Paired two-sided permutation <i>t</i> test	0.0001***; 0.23; 0.3		
	Forced: change rate (on-off)				
	M2-LS: 1.0 ± 0.2 vs controls: -0.2 ± 0.2	Unpaired two-sided permutation <i>t</i> test	0.0016**		
	M1-LS: 0.7 ± 0.6 vs controls: -0.2 ± 0.2	Unpaired two-sided permutation <i>t</i> test	0.11		
Data related to Extended Data Figure 4-1	Performance	Mean ± SEM (%)			
		Forced off vs forced on			
		M2-LS: 0.7 ± 0.7 vs 6 ± 3; M1-LS: 2.7 ± 1 vs 13 ± 5; controls: 1 ± 1 vs 1 ± 0.7	Paired two-sided permutation <i>t</i> test	0.1; 0.06; 0.8	
		Forced: change rate (on-off)			
	Inhibition before	M2-LS: 5.7 ± 2.9 vs controls: -0.06 ± 1	Unpaired two-sided permutation <i>t</i> test	0.11	
		M1-LS: 10.7 ± 5.4 vs controls: -0.06 ± 1.9	Unpaired two-sided permutation <i>t</i> test	0.04*	
		Data presented in the figure			
		Forced vs self-paced	Mann-Whitney <i>U</i> test	0.0001***	C57BL6/J mice (WT)
	Breaks S1 before	Forced vs S-P-break errors		0.32	AAV-Synapsine-Arch-M2-LS: <i>n</i> = 8
		Mean ± SEM (s)			Control group <i>n</i> = 16
		Forced off vs forced on			
		LS: 2.5 ± 0.2 vs 4.2 ± 0.6; controls: 2.5 ± 0.3 vs 2.1 ± 0.33	Paired two-sided permutation <i>t</i> test	0.02*; 0.3	
	Breaks S2 before	Forced: change rate (on-off)			
		LS: 1.6 ± 0.8 vs controls: -0.3 ± 0.2	Mann-Whitney <i>U</i> test	0.003**	
		Mean ± SEM (%)			
		Forced off vs forced on			
	Long-S1 sequences before	LS: 7.4 ± 4 vs 9 ± 4; controls: 0.8 ± 0.8 vs 1.8 ± 0.8	Paired two-sided permutation <i>t</i> test	0.38; 0.55	
		Forced: change rate (on-off)			
		LS: 2 ± 2 vs controls: 0.9 ± 1.3	Unpaired two-sided permutation <i>t</i> test	0.67	
		Mean ± SEM (%)			
Inhibition before	Forced off vs forced on				
	LS: 20 ± 6.2 vs 11 ± 3.7; controls: 17.7 ± 3.4 vs 14.9 ± 2.4	Paired two-sided permutation <i>t</i> test	0.06; 0.29		
	Forced: change rate (on-off)				
	LS: -8.7 ± 3 vs controls: -2 ± 2.5	Unpaired two-sided permutation <i>t</i> test	0.20		
Long-S1 sequences before	Mean ± SEM (%)				
	Forced off vs forced on				
	LS: 0 ± 0 vs 1.1 ± 1; controls: 1.8 ± 1 vs 0.9 ± 0.5	Paired two-sided permutation <i>t</i> test	1.0; 0.51		
	Forced: change rate (on-off)				
	Long-S1 sequences before	LS: 1.1 ± 1 vs controls: -0.8 ± 1.1	Unpaired two-sided permutation <i>t</i> test	0.36	

(Continued)

**Table 1: Continued**

Panel/data	Descriptive statistics	Type of test	<i>p</i> value	<i>n</i>
Transition	Mean ± SEM (s)			
Inhibition before	Forced off vs forced on LS: 1.1 ± 0.1 vs 1.0 ± 0.09; controls: 1.0 ± 0.1 vs 1.0 ± 0.1	Paired two-sided permutation <i>t</i> test	0.69; 0.78	
	Forced: change rate (on-off) LS: -0.06 ± 0.1 vs controls: 0 ± 0.03	Unpaired two-sided permutation <i>t</i> test	0.54	
Presses	Mean ± SEM (# presses)			
Inhibition before	Forced off vs forced on LS: 7.6 ± 0.09 vs 7.7 ± 0.08; controls: 8.0 ± 0.1 vs 7.9 ± 0.09	Paired two-sided permutation <i>t</i> test	0.05; 0.46	
	Forced: change rate (on-off) LS: 0.1 ± 0.06 vs controls: -0.08 ± 0.1	Unpaired two-sided permutation <i>t</i> test	0.127	
Latency	Mean ± SEM (s)			
Inhibition execution	Forced off vs forced on LS: 1.6 ± 0.1 vs 1.4 ± 0.1; controls: 2.6 ± 0.2 vs 3.1 ± 0.2	Paired two-sided permutation <i>t</i> test	0.01*; 0.04*	
	Forced: change rate (on-off) LS: -0.2 ± 0.1 vs controls: 0.5 ± 0.1	Unpaired two-sided permutation <i>t</i> test	0.001**	
Breaks S1	Mean ± SEM (%)			
Inhibition execution	Forced off vs forced on LS: 2.9 ± 1.4 vs 6.6 ± 2.8; controls: 1.4 ± 0.6 vs 1.8 ± 0.9	Paired two-sided permutation <i>t</i> test	0.38; 0.74	
	Forced: change rate (on-off) LS: 3.6 ± 3 vs controls: 0.4 ± 0.9	Unpaired two-sided permutation <i>t</i> test	0.30	
Breaks S2	Mean ± SEM (%)			
Inhibition execution	Forced off vs forced on LS: 17.7 ± 4 vs 22.5 ± 5.8; controls: 19.9 ± 2.7 vs 18.8 ± 3.5	Paired two-sided permutation <i>t</i> test	0.48; 0.78	
	Forced: change rate (on-off) LS: 4.8 ± 6 vs controls: -1.1 ± 4.2	Mann-Whitney <i>U</i> test	0.44	
Long-S1 sequences	Mean ± SEM (%)			
Inhibition execution	Forced off vs forced on LS: 0.7 ± 0.7 vs 0.8 ± 0.8; controls: 0.2 ± 0.2 vs 1.0 ± 0.8	Paired two-sided permutation <i>t</i> test	0.50; 1.0	
	Forced: change rate (on-off) LS: 0.1 ± 1.2 vs controls: 0.8 ± 0.5	Unpaired two-sided permutation <i>t</i> test	0.52	
Transition	Mean ± SEM (s)			
Inhibition execution	Forced off vs forced on LS: 1.0 ± 0.1 vs 1.0 ± 0.07; controls: 1.1 ± 0.12 vs 1.1 ± 0.1	Paired two-sided permutation <i>t</i> test	0.83; 0.39	
	Forced: change rate (on-off) LS: 0.01 ± 0.07 vs controls: 0.04 ± 0.04	Unpaired two-sided permutation <i>t</i> test	0.72	
Presses	Mean ± SEM (# presses)			
Inhibition execution	Forced off vs forced on LS: 7.6 ± 0.08 vs 7.6 ± 0.1; controls: 7.6 ± 0.04 vs 7.7 ± 0.06	Paired two-sided permutation <i>t</i> test	0.54; 0.78	
	Forced: change rate (on-off) LS: -0.09 ± 0.1 vs controls: 0.02 ± 0.07	Unpaired two-sided permutation <i>t</i> test	0.47	
Latency	Mean ± SEM (s)			
Inhibition transition	Forced off vs forced on LS: 1.9 ± 0.2 vs 1.8 ± 0.2; controls: 3.2 ± 0.3 vs 3 ± 0.3	Paired two-sided permutation <i>t</i> test	0.45; 0.34	
	Forced change rate (on-off) LS: -0.1 ± 0.1 vs controls: -0.1 ± 0.1	Unpaired two-sided permutation <i>t</i> test	0.82	
Breaks S1	Mean ± SEM (%)			
Inhibition transition	Forced off vs forced on LS: 0.6 ± 0.6 vs 5.5 ± 2.3; controls: 0 ± 0 vs 0.4 ± 0.4	Paired two-sided permutation <i>t</i> test	0.06; 1.0	
	Forced: change rate (on-off) LS: 4.8 ± 2.4 vs controls: 0.4 ± 0.4	Unpaired two-sided permutation <i>t</i> test	0.01*	
Breaks S2	Mean ± SEM (%)			
Inhibition transition	Forced off vs forced on LS: 16.8 ± 3.2 vs 15.9 ± 3.6; controls: 24.3 ± 3.9 vs 25.4 ± 4.4	Paired two-sided permutation <i>t</i> test	0.87; 0.82	
	Forced: change rate (on-off) LS: -0.8 ± 5 vs controls: 1 ± 4	Unpaired two-sided permutation <i>t</i> test	0.80	
Long-S1 sequences	Mean ± SEM (%)			
Inhibition transition	Forced off vs forced on LS: 1.7 ± 1.7 vs 0.5 ± 0.5; controls: 3.5 ± 0.02 vs 6.2 ± 0.2	Paired two-sided permutation <i>t</i> test	0.50; 0.21	
	Forced: change rate (on-off) LS: -1.2 ± 1.9 vs controls: 2.7 ± 1.9	Unpaired two-sided permutation <i>t</i> test	0.17	

(Continued)

**Table 1: Continued**

	Panel/data	Descriptive statistics	Type of test	<i>p</i> value	<i>n</i>
	Transition	Mean ± SEM (s)			
	Inhibition transition	Forced off vs forced on LS: 0.8 ± 0.07 vs 0.9 ± 0.08; controls: 1.2 ± 0.1 vs 1.2 ± 0.1	Paired two-sided permutation <i>t</i> test	0.02*; 0.16	
		Forced: change rate (on-off) LS: 0.1 ± 0.04 vs controls: -0.03 ± 0.02	Unpaired two-sided permutation <i>t</i> test	0.0006***	
	Presses	Mean ± SEM (# presses)			
	Inhibition transition	Forced off vs forced on LS: 7.7 ± 0.04 vs 7.5 ± 0.1; controls: 7.8 ± 0.1 vs 7.9 ± 0.1	Paired two-sided permutation <i>t</i> test	0.16; 0.41	
		Forced: change rate (on-off) LS: -0.1 ± 0.1 vs controls: 0.1 ± 0.1	Unpaired two-sided permutation <i>t</i> test	0.18	
Data related to Figure 5	Breaks S1	Mean ± SEM (%) Forced off vs forced on M2-LS: 0 ± 0 vs 0 ± 0; M1-LS: 1.3 ± 0.9 vs 1.2 ± 0.8; controls: 0.8 ± 0.5 vs 0.8 ± 0.8	Paired two-sided permutation <i>t</i> test	1.0; 0.7; 0.5	Emx1-cre mice (+/-) AAV-Arch-M2-LS: <i>n</i> = 9
		Forced: change rate (on-off) M2-LS: 0 ± 0 vs controls: 0.05 ± 0.6 M1-LS: -0.1 ± 1.1 vs controls: 0.05 ± 0.6	Unpaired two-sided permutation <i>t</i> test	0.5 0.9	AAV-Arch-M1-LS: <i>n</i> = 8 AAV-eYFP-M2-LS: <i>n</i> = 9 (controls)
	Breaks S2	Mean ± SEM (%) Forced off vs forced on M2-LS: 15 ± 5 vs 16 ± 3; M1-LS: 18.9 ± 3.6 vs 15.9 ± 3.5; controls: 20 ± 3.8 vs 21 ± 5	Paired two-sided permutation <i>t</i> test	0.8;0.6;0.9	
		Forced: change rate (on-off) M2-LS: 0.6 ± 4 vs controls: 0.6 ± 6 M1-LS: -3 ± 5 vs controls: 0.6 ± 6	Unpaired two-sided permutation <i>t</i> test	1.0 0.6	
	Sequence	Mean ± SEM (# presses) Forced off vs forced on M2-LS: 8.0 ± 0.2 vs 8.0 ± 0.1; M1-LS: 7.7 ± 0.1 vs 7.8 ± 0.1; controls: 7.7 ± 0.1 vs 7.6 ± 0.09	Paired two-sided permutation <i>t</i> test	0.43;0.67;0.33	
		Forced: change rate (on-off) M2-LS: 0.07 ± 0.08 vs controls: -0.1 ± 0.1 M1-LS: 0.04 ± 0.9 vs controls: -0.1 ± 0.1	Unpaired two-sided permutation <i>t</i> test	0.19 0.29	
	Long-S1 sequences	Mean ± SEM (%) Forced off vs forced on M2-LS: 4.2 ± 3.6 vs 3.1 ± 2.3; M1-LS: 4.5 ± 1.9 vs 1.7 ± 1.2; controls: 2.6 ± 2.6 vs 2.6 ± 2	Paired two-sided permutation <i>t</i> test	0.5;1.0; 1.0	
		Forced: change rate (on-off) M2-LS: -1 ± 1.7 vs controls: 0.9 ± 0.02 M1-LS: -2.8 ± 1.2 vs controls: 0 ± 0.8	Unpaired two-sided permutation <i>t</i> test	0.63 0.05	
	Duration	Mean ± SEM (s) Forced off vs forced on M2-LS: 5.19 ± 0.7 vs 4.7 ± 0.5; M1-LS: 4.1 ± 0.4 vs 4.22 ± 0.5; controls: 4.3 ± 1.0 vs 3.9 ± 0.6	Paired two-sided permutation <i>t</i> test	0.33;0.91;0.47	
		Self-paced off vs self-paced on M2-LS: 6.1 ± 0.7 vs 7.3 ± 1.5; M1-LS: 6.0 ± 0.5 vs 6.0 ± 0.4; controls: 5.8 ± 1.2 vs 5.1 ± 0.9		0.50;0.82;0.09	
		Forced: change rate (on-off) M2-LS: -0.4 ± 0.4 vs controls: -0.4 ± 0.4 M1-LS: 0.03 ± 0.4 vs controls: -0.4 ± 0.5	Unpaired two-sided permutation <i>t</i> test	0.91;0.44 0.18;0.20	
		Self-paced: change rate (on-off) M2-LS: 1.15 ± 1.2 vs controls: 1.0 ± 0.3 M1-LS: -0.05 ± 0.2 vs controls: 1.0 ± 0.3			
Data related to Figure 6	Transition	Mean ± SEM (s) Forced off vs forced on M2-LS: 1.0 ± 0.1 vs 1.0 ± 0.1; M1-LS: 1.2 ± 0.2 vs 1.1 ± 0.1; controls: 0.9 ± 0.1 vs 0.9 ± 0.1	Paired two-sided permutation <i>t</i> test	0.21; 0.55; 0.8	Emx1-cre mice (+/-) AAV-Arch-M2-LS: <i>n</i> = 9 AAV-Arch-M1-LS: <i>n</i> = 8
		Forced: change rate (on-off) M2-LS: -0.04 ± 0.03 vs controls: 0 ± 0.02 M1-LS: -0.1 ± 0.14 vs controls: 0 ± 0.02	Unpaired two-sided permutation <i>t</i> test	0.34 0.59	AAV-eYFP-M2-LS: <i>n</i> = 9 (controls)

(Continued)

Table 1: Continued

Panel/data	Descriptive statistics	Type of test	<i>p</i> value	<i>n</i>
Breaks S1	Mean ± SEM (%)			
	Forced off vs forced on	Paired two-sided permutation <i>t</i> test	1.0; 1.0; 1.0	
	M2-LS: 0 ± 0 vs 0 ± 0; M1-LS: 2.1 ± 1 vs 0 ± 0; controls: 0 ± 0 vs 0 ± 0			
	Forced: change rate (on-off)			
Breaks S2	Mean ± SEM (%)			
	Forced off vs forced on	Paired two-sided permutation <i>t</i> test	0.49; 0.24; 0.70	
	M2-LS: 15 ± 4.6 vs 18 ± 4.4; M1-LS: 18 ± 4.8 vs 12 ± 3; controls: 24 ± 5 vs 22 ± 3			
	Forced: change rate (on-off)			
Duration	Mean ± SEM (s)			
	Forced off vs forced on	Paired two-sided permutation <i>t</i> test	0.12; 0.46; 0.70	
	M2-LS: 4.8 ± 0.3 vs 4.1 ± 0.3; M1-LS: 3.8 ± 0.4 vs 3.9 ± 0.4; controls: 3.4 ± 0.4 vs 3.8 ± 0.4			
	Self-paced off vs self-paced on		0.23; 0.69; 0.08	
# Presses sequences	Mean ± SEM (# presses)			
	Forced off vs forced on	Paired two-sided permutation <i>t</i> test	0.14; 0.67; 0.19	
	M2-LS: 7.9 ± 0.2 vs 7.7 ± 0.07; M1-LS: 7.7 ± 0.07 vs 7.8 ± 0.05; controls: 7.8 ± 0.2 vs 8.0 ± 0.2			
	Self-paced off vs self-paced on		0.27; 0.97; 0.25	
	M2-LS: 10.9 ± 0.6 vs 11.9 ± 0.7; M1-LS: 11.8 ± 0.7 vs 11.8 ± 0.5; controls: 11.1 ± 0.3 vs 10.7 ± 0.4			
	Forced: change rate (on-off)			
	M2-LS: -0.2 ± 0.1 vs controls: 0.1 ± 0.1	Unpaired two-sided permutation <i>t</i> test	0.049*; 0.55	
	M1-LS: 0.05 ± 0.08 vs controls: 0.1 ± 0.1			
	Self-paced: change rate (on-off)		0.14; 0.57	
	M2-LS: 2.4 ± 1.7 vs controls: -0.2 ± 0.1			
	M1-LS: -0.08 ± 0.2 vs controls: -0.2 ± 0.1			
	M2-LS: 1.0 ± 0.8 vs controls: -0.3 ± 0.3		0.11; 0.37	
M1-LS: 0.01 ± 0.2 vs controls: -0.3 ± 0.3				

this last difference is that M2→LS activity may be required to set the execution of sequences by impinging on specific striatal subcircuits (Wall et al., 2013). However, our direct inhibition of the LS did not differentiate between striatal subcircuits. To address this, Extended Data Figure 4-3 shows that the M2→LS innervates, strongly the striatal projection neurons from the direct pathway. Such preferential innervation has been previously suggested (Wall et al., 2013; Nelson et al., 2020) to direct the structuring of sequences in serial order tasks (Rothwell et al., 2015), although only after learning.

Lastly, the quantification of the cells that project from M2/M1 to other brain areas by crossing through the LS showed it to be a small percentage of neurons (M2/M1→Str→Th 3%; M2/M1→Str→Pns 3%; Extended Data Fig. 4-2). This data, plus the evidence that Arch3.0 mainly has inhibitory actions through local inhibition rather than affecting the propagation of action potentials (El-Gaby et al., 2016), suggests that the effects observed here were

predominantly from optogenetic inhibition of the cortico-striatal projections from M2 or M1 into the LS.

In conclusion, this study shows that the premotor cortico-striatal projections to the LS contribute to the initiation and execution of self-paced sequences. It supports a model in which both M2 and M1 contain activity modulated by sequence initiation and execution. However, the M2→LS cortico-striatal projections mainly contribute to the proper execution/structuring of self-paced sequences. Both, M2 and M1 cortico-striatal projections contribute to the initiation of sequences. Also, our findings support the idea that the premotor cortico-striatal projections to the LS are a serial driver for the execution of sequences (Lashley, 1951; Zeigler and Gallistel, 1981; Graybiel, 1998; Rosenbaum et al., 2007; Jin and Costa, 2015). Altogether the presented findings may have important implications for pathophysiological conditions whereby self-paced generation of actions is impaired.

## References

- Bartolo R, Merchant H (2015)  $\beta$  Oscillations are linked to the initiation of sensory-cued movement sequences and the internal guidance of regular tapping in the monkey. *J Neurosci* 35:4635–4640.
- Bartolo R, Prado L, Merchant H (2014) Information processing in the primate basal ganglia during sensory-guided and internally driven rhythmic tapping. *J Neurosci* 34:3910–3923.
- Berlot E, Popp NJ, Grafton ST, Diedrichsen J (2021) Combining repetition suppression and pattern analysis provides new insights into the role of M1 and parietal areas in skilled sequential actions. *J Neurosci*. Advance online publication. Retrieved Jul 26, 2021. doi: 10.1523/JNEUROSCI.0863-21.2021.
- Burguière E, Monteiro P, Feng G, Graybiel AM (2013) Optogenetic stimulation of lateral orbitofronto-striatal pathway suppresses compulsive behaviors. *Science* 340:1243–1246.
- Chen PY, Popovich PM (2011) Correlation: parametric and nonparametric measures. Beverly Hills: Sage University Papers Series on Quantitative Applications in the Social Sciences.
- Churchland MM, Santhanam G, Shenoy KV (2006) Preparatory activity in premotor and motor cortex reflects the speed of the upcoming reach. *J Neurophysiol* 96:3130–3146.
- Crowe DA, Zarco W, Bartolo R, Merchant H (2014) Dynamic representation of the temporal and sequential structure of rhythmic movements in the primate medial premotor cortex. *J Neurosci* 34:11972–11983.
- Cui G, Jun SB, Jin X, Pham MD, Vogel SS, Lovinger DM, Costa RM (2013) Concurrent activation of striatal direct and indirect pathways during action initiation. *Nature* 494:238–242.
- Dhawale AK, Wolff SBE, Raymond K, Ölveczky BP (2021) The basal ganglia control the detailed kinematics of learned motor skills. *Nat Neurosci* 24:1256–1269.
- Díaz-Hernández E, Contreras-López R, Sánchez-Fuentes A, Rodríguez-Sibrian L, Ramírez-Jarquín JO, Tecuapetla F (2018) The thalamostriatal projections contribute to the initiation and execution of a sequence of movements. *Neuron* 100:739–752.e5.
- Donoghue JP, Wise SP (1982) The motor cortex of the rat: Cytoarchitecture and microstimulation mapping. *J Comp Neurol* 212:76–88.
- El-Gaby M, Zhang Y, Wolf K, Schwiening CJ, Paulsen O, Shipton OA (2016) Archaelhodopsin selectively and reversibly silences synaptic transmission through altered pH. *Cell Rep* 16:2259–2268.
- Friedman A, Homma D, Gibb LG, Amemori K, Rubin SJ, Hood AS, Riad MH, Graybiel AM (2015) A corticostriatal path targeting striosomes controls decision-making under conflict. *Cell* 161:1320–1333.
- Fujii N, Graybiel AM (2005) Time-varying covariance of neural activities recorded in striatum and frontal cortex as monkeys perform sequential-saccade tasks. *Proc Natl Acad Sci USA* 102:9032–9037.
- Geddes CE, Li H, Jin X (2018) Optogenetic editing reveals the hierarchical organization of learned action sequences article optogenetic editing reveals the hierarchical organization of learned action sequences. *Cell* 174:32–43.
- Gorski JA, Talley T, Qiu M, Puelles L, Rubenstein JLR, Jones KR (2002) Cortical excitatory neurons and glia, but not GABAergic neurons, are produced in the Emx1-expressing lineage. *J Neurosci* 22:6309–6314.
- Graybiel AM (1998) The basal ganglia and chunking of action repertoires. *Neurobiol Learn Mem* 70:119–136.
- Guo H, Hong S, Jin XL, Chen RS, Avasthi PP, Tu YT, Ivancov TL, Li Y (2000) Specificity and efficiency of Cre-mediated recombination in Emx1-cre knock-in mice. *Biochem Biophys Res Commun* 273:661–665.
- Hernández A, Náchter V, Luna R, Zainos A, Lemus L, Alvarez M, Vázquez Y, Camarillo L, Romo R (2010) Decoding a perceptual decision process across cortex. *Neuron* 66:300–314.
- Hikosaka O, Isoda M (2010) Switching from automatic to controlled behavior: cortico-basal ganglia mechanisms. *Trends Cogn Sci* 14:154–161.
- Hintiryan H, Foster NN, Bowman I, Bay M, Song MY, Gou L, Yamashita S, Bienkowski MS, Zingg B, Zhu M, Yang XW, Shih JC, Toga AW, Dong HW (2016) The mouse cortico-striatal projectome. *Nat Neurosci* 19:1100–1114.
- Ho J, Tumkaya T, Sameer A, Choi H, Claridge A (2019) Moving beyond p values: data analysis with estimation graphics. *Nat Methods* 16:565–566.
- Hunnicutt BJ, Jongbloets BC, Birdsong WT, Gertz KJ, Zhong H, Mao T (2016) A comprehensive excitatory input map of the striatum reveals novel functional organization. *Elife* 5:e19103.
- Inase M, Sakai ST, Tanji J (1996) Overlapping corticostriatal projections from the supplementary motor area and the primary motor cortex in the macaque monkey: an anterograde double labeling study. *J Comp Neurol* 373:283–296.
- Jin X, Costa RM (2015) Shaping action sequences in basal ganglia circuits. *Curr Opin Neurobiol* 33:188–196.
- Jin DZ, Fujii N, Graybiel AM (2009) Neural representation of time in cortico-basal ganglia circuits. *Proc Natl Acad Sci USA* 106:19156–19161.
- Jin X, Tecuapetla F, Costa RM (2014) Basal ganglia subcircuits distinctively encode the parsing and concatenation of action sequences. *Nat Neurosci* 17:423–430.
- Kawai R, Markman T, Poddar R, Ko R, Fantana AL, Dhawale AK, Kampff AR, Ölveczky BP (2015) Motor cortex is required for learning but not for executing a motor skill. *Neuron* 86:800–812.
- Kobak D, Brendel W, Constantinidis C, Feierstein CE, Kepecs A, Mainen ZF, Qi XL, Romo R, Uchida N, Machens CK (2016) Demixed principal component analysis of neural population data. *Elife* 5:e10989.
- Kupferschmidt DA, Juczewski K, Cui G, Johnson KA, Lovinger DM (2017) Parallel, but dissociable, processing in discrete corticostriatal inputs encodes skill learning. *Neuron* 96:476–489.e5.
- Kurata K, Tanji J (1985) Contrasting neuronal activity in supplementary and precentral motor cortex of monkeys. II Responses to movement triggering vs. nontriggering sensory signals. *J Neurophysiol* 53:142–152.
- Lashley K (1951) The problem of serial order in behavior. In: *Cerebral mechanisms in behavior* (Jeffress LA, ed), pp 112–136. New York: Wiley.
- Li N, Daie K, Svoboda K, Druckmann S (2016) Robust neuronal dynamics in premotor cortex during motor planning. *Nature* 532:459–464.
- Lima SQ, Hromádka T, Znamenskiy P, Zador AM (2009) PINP: a new method of tagging neuronal populations for identification during in vivo electrophysiological recording. *PLoS One* 4:e6099.
- Lucchetti C, Bon L (2001) Time-modulated neuronal activity in the premotor cortex of macaque monkeys. *Exp Brain Res* 141:254–260.
- Mahn M, Prigge M, Ron S, Levy R, Yizhar O (2016) Biophysical constraints of optogenetic inhibition at presynaptic terminals. *Nat Neurosci* 19:554–556.
- Manouze H, Ghestem A, Poillat V, Bennis M, Ba-M'hamed S, Benoliel JJ, Becker C, Bernard C (2019) Effects of single cage housing on stress, cognitive, and seizure parameters in the rat and mouse pilocarpine models of epilepsy. *eNeuro* 6:ENEURO.0179-18.2019.
- Martiros N, Burgess AA, Graybiel AM (2018) Inversely active striatal projection neurons and interneurons selectively delimit useful behavioral article inversely active striatal projection neurons and interneurons selectively delimit useful behavioral sequences. *Curr Biol* 28:560–573.
- Mendoza G, Méndez JC, Pérez O, Prado L, Merchant H (2018) Neural basis for categorical boundaries in the primate pre-SMA during relative categorization of time intervals. *Nat Commun* 9:1098.
- Merchant H, Pérez O, Zarco W, Gámez J (2013) Interval tuning in the primate medial premotor cortex as a general timing. *J Neurosci* 33:9082–9096.

- Murakami M, Vicente MI, Costa GM, Mainen ZF (2014) Neural antecedents of self-initiated actions in secondary motor cortex. *Nat Neurosci* 17:1574–1582.
- Mushiake H, Inase M, Tanji J (1990) Selective coding of motor sequence in the supplementary motor area of the monkey cerebral cortex. *Exp Brain Res* 82:208–210.
- Nakayama Y, Yamagata T, Tanji J, Hoshi E (2008) Transformation of a virtual action plan into a motor plan in the premotor cortex. *J Neurosci* 28:10287–10297.
- Nakayama H, Ibañez-Tallon I, Heintz N (2018) Cell-type-specific contributions of medial prefrontal neurons to flexible behaviors. *J Neurosci* 38:4490–4504.
- Nelson A, Abdelmesih B, Costa RM (2020) Corticospinal neurons encode complex motor signals that are broadcast to dichotomous striatal circuits. *bioRxiv* 2020.08.31.275180.
- Oh SW, Harris JA, Ng L, Winslow B, Cain N, Mihalas S, Wang Q, Lau C, Kuan L, Henry AM, Mortrud MT, Ouellette B, Nguyen TN, Sorensen SA, Slaughterbeck CR, Wakeman W, Li Y, Feng D, Ho A, Nicholas E, et al. (2014) A mesoscale connectome of the mouse brain. *Nature* 508:207–214.
- Passingham RE, Myers C, Rawlins N, Lightfoot V, Fearn S (1988) Premotor cortex in the rat. *Behav Neurosci* 102:101–109.
- Redgrave P, Rodriguez M, Smith Y, Rodriguez-Oroz MC, Lehericy S, Bergman H, Agid Y, DeLong MR, Obeso JA (2010) Goal-directed and habitual control in the basal ganglia: implications for Parkinson's disease. *Nat Rev Neurosci* 11:760–772.
- Riehle A, Requin J (1989) Monkey primary motor and premotor cortex: single-cell activity related to prior information about direction and extent of an intended movement. *J Neurophysiol* 61:534–549.
- Riehle A, MacKay WA, Requin J (1994) Are extent and force independent movement parameters? Preparation- and movement-related neuronal activity in the monkey cortex. *Exp Brain Res* 99:56–74.
- Romo R, Schultz W (1987) Neuronal activity preceding self-initiated or externally timed arm movement in area 6 of monkey cortex. *Exp Brain Res* 67:656–602.
- Romo R, Schultz W (1992) Role of primate basal ganglia and frontal cortex in the internal generation of movements. *Exp Brain Res* 91:396–407.
- Rosenbaum DA, Cohen RG, Jax SA, Weiss DJ, Van Der Wel R (2007) The problem of serial order in behavior: Lashley's legacy. *Hum Mov Sci* 26:525–554.
- Rothwell PE, Hayton SJ, Sun GL, Fuccillo MV, Lim BK, Malenka RC (2015) Input- and output-specific regulation of serial order performance by corticostriatal circuits. *Neuron* 88:345–356.
- Sakurai Y, Takahashi S, Inoue M (2004) Stimulus duration in working memory is represented by neuronal activity in the monkey prefrontal cortex. *Eur J Neurosci* 20:1069–1080.
- Shima K, Tanji J (2000) Neuronal activity in the supplementary and presupplementary motor areas for temporal organization of multiple movements neuronal activity in the supplementary and presupplementary motor areas for temporal organization of multiple movements. *J Neurophysiol* 84:2148–2160.
- Shima K, Isoda M, Mushiake H, Tanji J (2007) Categorization of behavioural sequences in the prefrontal cortex. *Nature* 445:315–318.
- Siniscalchi MJ, Phoumthippavong V, Ali F, Lozano M, Kwan AC (2016) Fast and slow transitions in frontal ensemble activity during flexible sensorimotor behavior. *Nat Neurosci* 19:1234–1242.
- Smith KS, Graybiel AM (2013) A dual operator view of habitual behavior reflecting cortical and striatal dynamics. *Neuron* 79:361–374.
- Sohur US, Padmanabhan HK, Kotchetkov IS, Menezes JRL, Macklis JD (2014) Anatomic and molecular development of corticostriatal projection neurons in mice. *Cereb Cortex* 24:293–303.
- Storey JD (2002) A direct approach to false discovery rates. *J R Stat Soc Series B Stat Methodol* 64:479–498.
- Tanji J, Evarts EV (1976) Anticipatory activity of motor cortex neurons in relation to direction of an intended movement. *J Neurophysiol* 39:1062–1068.
- Tecuapetla F, Jin X, Lima SQ, Costa RM (2016) Complementary contributions of striatal projection pathways to action initiation and execution. *Cell* 166:703–715.
- Thaler DE, Rolls ET, Passingham RE (1988) Neuronal activity of the supplementary motor area (SMA) during internally and externally triggered wrist movements. *Neurosci Lett* 93:264–269.
- Wall NR, De La Parra M, Callaway EM, Kreitzer AC (2013) Differential innervation of direct- and indirect-pathway striatal projection neurons. *Neuron* 79:347–360.
- Wilson CJ (1989) The basal ganglia. In: *The synaptic organization of the brain*, Ed 3 (Shepherd GM, ed), pp 279–316. Oxford: Oxford University Press.
- Zeigler HP, Gallistel CR (1981) The organization of action: a new synthesis. *Am J Psychol* 94:190.